MCF-7, which expressed aromatase mRNA, but not that of aromatase negative normal MCF-12A epithelial cells [40]. Furthermore, concurrent treatment of MCF-7 cells with estradiol in the presence of letrozole significantly suppressed the estradiol induced increment of matrix metalloproteinase level [40]. These findings also suggest that aromatase play an important role of estrogen-dependent pathway in breast parenchymal or carcinoma cells as well as stromal cells.

## 4. Conclusion: intracrine "paracrine versus autocrine" in breast carcinomas

Hormones which are released from one cell and reach nearby target cells by diffusion through the extracellular space are called *paracrine*. Hormones may also act on the cells that produced them, in which case they are called *autocrine*. *In situ* formation of biologically active estrogen at the sites of their actions from biologically inactive precursors in the circulation termed *intracrine* (Fig. 3) have been demonstrated to play very important roles in hormone-dependent carcinomas. In this intracrine manner of breast carcinoma tissues, it is considered that there are two patterns of estrogen supplying systems (Fig. 3), i.e., estrogen releasing from stromal cell (*paracrine*) or carcinoma cell itself (*autocrine*). Parenchymal carcinoma cells are major cell types of human breast cancer tissues and estrogen produced *in situ* in carcinoma cells could reach estrogen receptor in carcinoma cells in a more effective manner with higher concentrations. Therefore, expression levels of aromatase per cells in carcinoma cells may be lower than those in stromal cells, but their contribution to intratumoral estrogen synthesis and subsequent estrogen-dependent cell proliferation is considered significant.

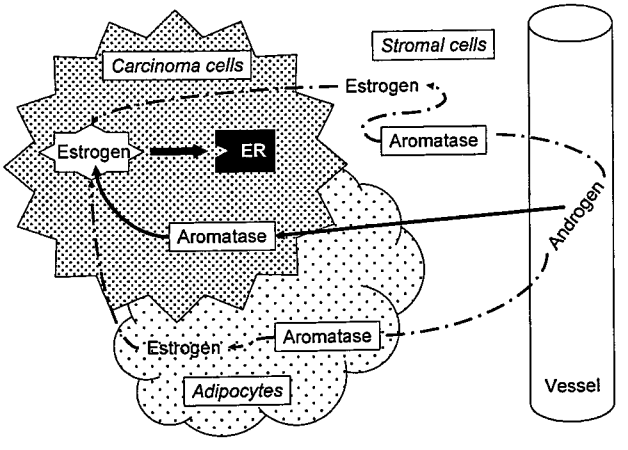


Fig. 3. Summary of intracrine of breast carcinoma tissues. There are two patterns of estrogen supplying systems, which are estrogen releasing from stromal cell (paracrine, dashed line) or carcinoma cell itself (autocrine, solid line), in postmenopausal breast carcinoma tissues. Estrogen synthesized by aromatase bonds to estrogen receptor (ER), which is located in carcinoma cells but not in stromal cells.

## References

[1] N. Fournet-Dulguerov, N.J. MacLusky, C.Z. Leranth, R. Todd, C.R. Mendelson, E.R. Simpson, F. Naftolin, Immunohistochemical localization of aromatase cytochrome P-450 and estradiol dehydrogenase in the syncytiotrophoblast of the human placenta, J. Clin. Endocrinol. Metab. 65 (1987) 757–764.
[2] A. Conley, M. Hinshelwood, Mammalian aromatase, Reproduction 121 (2001) 685–695.
[3] C. Longcope, J.H. Pratt, S.H. Schneider, S.E. Fineberg, Aromatization of androgens by muscle and adipose tissue *in vivo*, J. Clin. Endocrinol. Metab. 46 (1978) 146–152.
[4] H. Sasano, M. Uzuki, T. Sawai, H. Nagura, G. Matsunaga, O. Kashimoto, N. Harada, Aromatase in human bone tissue, J. Bone Miner. Res. 12 (1997) 1416–1423.
[5] H.U. Schweikert, L. Milewich, J.D. Wilson, Aromatization of androstenedione by cultured human fibroblasts, J. Clin. Endocrinol. Metab. 43 (1976) 785–795.
[6] H. Murakami, N. Harada, H. Sasano, Aromatase in atherosclerotic lesions of human aorta, J. Steroid Biochem. Mol. Biol. 79 (2001) 67–74.
[7] F.L. Bellino, Y. Osawa, Localization of estrogen synthetase in the chorionic villus fraction after homogenization of human term placenta, J. Clin. Endocrinol. Metab. 44 (1997) 699–707.
[8] H. Sasano, H. Nagura, N. Harada, Y. Goukon, M. Kimura, Immunolocalization of aromatase and other steroidogenic enzymes in human breast disorders, Hum. Pathol. 25 (1994) 530–535.
[9] H. Sasano, N. Harada, Intratumoral aromatase in human breast, endometrial, and ovarian malignancies, Endocr. Rev. 19 (1998) 593–607.
[10] K. Watanabe, H. Sasano, N. Harada, M. Ozaki, H. Niikura, S. Sato, A. Yajima, Aromatase in human endometrial carcinoma and hyperplasia. Immunohistochemical, in situ hybridization, and biochemical studies, Am. J. Pathol. 146 (1995) 491–500.
[11] W.R. Miller, T.J. Anderson, W.J. Jack, Relationship between tumor aromatase activity, tumor characteristics and response to therapy, J. Steroid Biochem. Mol. Biol. 37 (1990) 1055–1059.
[12] M. Baum, A.U. Budzar, J. Cuzick, J. Forbes, J.H. Houghton, J.G. Klijn, T. Sahmoud, ATAC Trialists' Group, Anastrozole alone or in combination with tamoxifen versus tamoxifen alone for adjuvant treatment of postmenopausal women with early breast cancer: first results of the ATAC randomised trial, Lancet 359 (2002) 2131–2139.
[13] P.E. Goss, J.N. Ingle, S. Martino, N.J. Robert, H.B. Muss, M.J. Piccart, M. Castiglione, D. Tu, L.E. Shepherd, K.I. Pritchard, R.B. Livingston, N.E. Davidson, L. Norton, E.A. Perez, J.S. Abrams, P. Therasse, M.J. Palmer, J.L. Pater, A randomized trial of letrozole in postmenopausal women after five years of tamoxifen therapy for early-stage breast cancer, N. Engl. J. Med. 349 (2003) 1793–1802.
[14] R.C. Coombes, E. Hall, L.J. Gibson, R. Paridaens, J. Jassem, T. Delozier, S.E. Jones, I. Alvarez, G. Bertelli, O. Ortmann, A.S. Coates, E. Bajetta, D. Dodwell, R.E. Coleman, L.J. Fallowfield, E. Mickiewicz, J. Andersen, P.E. Lonning, G. Cocconi, A. Stewart, N. Stuart, C.F. Snowdon, M. Carpentieri, G. Massimini, J.M. Bliss, Intergroup Exemestane Study, a randomized trial of exemestane after two to three years of tamoxifen therapy in postmenopausal women with primary breast cancer, N. Engl. J. Med. 350 (2004) 1081–1092.
[15] R.J. Santen, J. Martel, M. Hoagland, F. Naftolin, L. Roa, N. Harada, L. Hafer, R. Zaino, S.J. Santner, Stromal spindle cells contain aromatase in human breast tumors, J. Clin. Endocrinol. Metab. 79 (1994) 627–632.
[16] J.M. Esteban, Z. Warsi, M. Haniu, P. Hall, J.E. Shively, S. Chen, Detection of intratumoral aromatase in breast carcinomas. An immunohistochemical study with clinicopathologic correlation, Am. J. Pathol. 140 (1992) 337–343.

[17] L.M. Berstein, A.A. Larionov, A.Sh. Kyshtoobaeva, K.M. Pozharisski, V.F. Semiglazov, O.A. Ivanova, Aromatase in breast cancer tissue—localization and relationship with reproductive status of patients, J. Cancer Res. Clin. Oncol. 122 (1996) 495–498.
[18] Q. Lu, J. Nakmura, A. Savinov, W. Yue, J. Weisz, D.J. Dabbs, G. Wolz, A. Brodie, Expression of aromatase protein and messenger ribonucleic acid in tumor epithelial cells and evidence of functional significance of locally produced estrogen in human breast cancers, Endocrinology 137 (1996) 3061–3068.
[19] K.C. Shenton, M. Dowsett, Q. Lu, A. Brodie, H. Sasano, N.P. Sacks, M.G. Rowlands, Comparison of biochemical aromatase activity with aromatase immunohistochemistry in human breast carcinomas, Breast Cancer Res. Treat. 49 (1998) S101–S107.
[20] A.M. Brodie, Q. Lu, B.J. Long, A. Fulton, T. Chen, N. Macpherson, P.C. DeJong, M.A. Blankenstein, J.W. Nortier, P.H. Slee, J. van de Ven, J.M. van Gorp, J.R. Elbers, M.E. Schipper, G.H. Blijham, J.H. Thijssen, Aromatase and COX-2 expression in human breast cancers, J. Steroid Biochem. Mol. Biol. 79 (2001) 41–47.
[21] Y. Tsunoda, Y. Shimizu, A. Tsunoda, K. Kamiya, M. Kusano, M. Takimoto, Breast carcinomas with immunocytochemical detection of aromatase in fine-needle aspirates: report of three cases, Hum. Pathol. 32 (2001) 348–351.
[22] Z. Zhang, H. Yamashita, T. Toyama, Y. Hara, Y. Omoto, H. Sugiura, S. Kobayashi, N. Harada, H. Iwase, Semi-quantitative immunohistochemical analysis of aromatase expression in ductal carcinoma in situ of the breast, Breast Cancer Res. Treat. 74 (2002) 47–53.
[23] H. Sasano, D.P. Edwards, T.J. Anderson, S.G. Silverberg, D.B. Evans, R.J. Santen, P. Ramage, E.R. Simpson, A.S. Bhatnagar, W.R. Miller, Validation of new aromatase monoclonal antibodies for immunohistochemistry: progress report, J. Steroid Biochem. Mol. Biol. 86 (2003) 239–244.
[24] H. Sasano, T.J. Anderson, S.G. Silverberg, R.J. Santen, M. Conway, D.P. Edwards, A. Krause, A.S. Bhatnagar, D.B. Evans, W.R. Miller, The validation of new aromatase monoclonal antibodies for immunohistochemistry—a correlation with biochemical activities in 46 cases of breast cancer, J. Steroid Biochem. Mol. Biol. 95 (2005) 35–39.
[25] T. Suzuki, Y. Miki, Y. Nakamura, T. Moriya, K. Ito, N. Ohuchi, H. Sasano, Sex steroid-producing enzymes in human breast cancer, Endocr. Relat. Cancer. 12 (2005) 701–720.
[26] M.R. Emmert-Buck, R.F. Bonner, P.D. Smith, R.F. Chuaqui, Z. Zhuang, S.R. Goldstein, R.A. Weiss, L.A. Liotta, Laser capture microdissection, Science 274 (1996) 998–1001.
[27] T. Suzuki, Y. Miki, T. Fukuda, T. Nakata, T. Moriya, H. Sasano, Analysis for localization of steroid sulfatase in human tissues, Meth. Enzymol. 400 (2005) 303–316.
[28] N. Harada, S. Honda, Molecular analysis of aberrant expression of aromatase in breast cancer tissues, Breast Cancer Res. Treat. 49 (1998) S15–S21.
[29] J.T. Sanderson, R.J. Letcher, M. Heneweer, J.P. Giesy, M. van den Berg, Effects of chloro-s-triazine herbicides and metabolites on aromatase activity in various human cell lines and on vitellogenin production in male carp hepatocytes, Environ. Health Perspect. 109 (2001) 1027–1031.
[30] J. Shields-Botella, G. Chetrite, S. Meschi, J.R. Pasqualini, Effect of nomegestrol acetate on estrogen biosynthesis and transformation in MCF-7 and T47-D breast cancer cells, J. Steroid Biochem. Mol. Biol. 93 (2005) 1–13.
[31] X.Z. Sun, D. Zhou, S. Chen, Autocrine and paracrine actions of breast tumor aromatase. A three-dimensional cell culture study involving aromatase transfected MCF-7 and T-47D cells, J. Steroid Biochem. Mol. Biol. 63 (1997) 29–36.
[32] C.M. Ryde, J.E. Nicholls, M. Dowsett, Steroid and growth factor modulation of aromatase activity in MCF7 and T47D breast carcinoma cell lines, Cancer Res. 52 (1992) 1411–1415.
[33] L.A. Castagnetta, O.M. Granata, V. Bellavia, R. Amodio, E. Scaccianoce, M. Notarbartolo, M.R. Follari, M.D. Miceli, G. Carruba, Product of aromatase activity in intact LNCaP and MCF-7 human cancer cells, J. Steroid Biochem. Mol. Biol. 61 (1997) 287–292.
[34] K. Sonne-Hansen, A.E. Lykkesfeldt, Endogenous aromatization of testosterone results in growth stimulation of the human MCF-7 breast cancer cell line, J. Steroid Biochem. Mol. Biol. 93 (2005) 25–34.
[35] C. Yang, D. Zhou, S. Chen, Modulation of aromatase expression in the breast tissue by ERR alpha-1 orphan receptor, Cancer Res. 58 (1998) 5695–5700.
[36] Y.M. Mu, T. Yanase, Y. Nishi, N. Hirase, K. Goto, R. Takayanagi, H. Nawata, A nuclear receptor system constituted by RAR and RXR induces aromatase activity in MCF-7 human breast cancer cells, Mol. Cell. Endocrinol. 166 (2000) 137–145.
[37] T. Suzuki, Y. Miki, T. Moriya, N. Shimada, T. Ishida, H. Hirakawa, N. Ohuchi, H. Sasano, Estrogen-related receptor alpha in human breast carcinoma as a potent prognostic factor, Cancer Res. 64 (2004) 4670–4676.
[38] T. Suzuki, T. Moriya, A. Sugawara, N. Ariga, H. Takabayashi, H. Sasano, Retinoid receptors in human breast carcinoma: possible modulators of in situ estrogen metabolism, Breast Cancer Res. Treat. 65 (2001) 31–40.
[39] N. Ariga, T. Moriya, T. Suzuki, M. Kimura, N. Ohuchi, H. Sasano, Retinoic acid receptor and retinoid X receptor in ductal carcinoma in situ and intraductal proliferative lesions of the human breast, Jpn. J. Cancer Res. 91 (2000) 1169–1176.
[40] T.N. Mitropoulou, G.N. Tzanakakis, D. Kletsas, H.P. Kalofonos, N.K. Karamanos, Letrozole as a potent inhibitor of cell proliferation and expression of metalloproteinases (MMP-2 and MMP-9) by human epithelial breast cancer cells, Int. J. Cancer 104 (2003) 155–160.

*Jpn J Clin Oncol 2007;37(4)250–255*
*doi:10.1093/jjco/hym021*

# Reliability of Prognostic Factors in Breast Carcinoma Determined by Core Needle Biopsy

**Shin Usami[1,2], Takuya Moriya[1], Masakazu Amari[2], Akihiko Suzuki[2], Takanori Ishida[2], Hironobu Sasano[1] and Noriaki Ohuchi[2]**

[1]Department of Pathology and [2]Breast and Endocrine Surgery, Tohoku University Hospital, Sendai, Japan

Received October 17, 2006; accepted November 22, 2006; published online May 7, 2007

**Objective:** The aim of this study was to evaluate the reliability of information obtained by core needle biopsy (CNB).
**Methods:** We studied 111 women (112 lesions) with breast cancer who underwent CNB and subsequent surgical excision. Six factors (histological type, nuclear grade, histological grade, estrogen receptor (ER) status, progesterone receptor (PR) status, and human epidermal growth factor receptor-2 (HER2) status) were evaluated in a blinded fashion at CNB and at surgical excision.
**Results:** The histological type at CNB correlated exactly with that of the excisional specimen in 83% (87/105) of the cases. Of the 45 *in situ* lesions at CNB, 16 (36%) were found to have invasive carcinoma at surgical excision. The difference between the specimens from CNB and those from surgery in terms of the absolute concordance rate and κ statistic value were 61% with a fair κ value (0.26) in the nuclear grade, 75% with a moderate κ value (0.55) in the histological grade, 95% with an almost perfect κ value (0.84) in ER, 88% with a substantial κ value (0.70) in PR and 88% with a substantial κ value (0.65) in HER2. Regarding the evaluation of nuclear and histological grades, a trend toward greater accuracy was observed when thicker specimens were used.
**Conclusions:** CNB provided reliable information on the histological type of invasive carcinoma. It also evaluated ER, PR and HER2 (only in cases where the score was 3+) accurately in spite of the limited quantity of the specimen obtained with the thin (16-gauge) needle.

*Key words: breast cancer – core needle biopsy – HER2 – hormone receptor – prognostic factor*

## BACKGROUND

Recently, core needle biopsy (CNB) has been widely used as an alternative to surgical open biopsy. There have been several studies on the diagnostic accuracy of CNB (1–6), which showed high diagnostic accuracy for both palpable and non-palpable breast lesions. One of the reasons for the preference of CNB over fine needle aspiration biopsy cytology (FNA) is that the incidence of ductal carcinoma *in situ* (DCIS) has increased among all breast cancers.

However, for therapeutic advancement in the treatment of breast cancer, many clinicians would like CNB to provide information not only on the histological diagnosis but also on various predictive factors because such information is very important when deciding the therapeutic strategy. Particularly in settings where neo-adjuvant therapy is used, such information would be unique to each patient because at the time of the operation, we cannot obtain the native tissue samples, i.e. those that have not been modified by the treatment. In addition, a recent study (7) on metastatic breast cancer has shown a high level of discordance for both the estrogen receptor (ER) and the progesterone receptor (PR) between primary and metastatic disease. This reinforces the importance of obtaining biopsy material at the first presentation of metastasis. Furthermore, survival after metastasis is related to the ER status of the metastatic tumor rather than that of the primary tumor. In clinical practice, material from metastatic lesions is often obtained by CNB.

There are few studies that detail the predictive factors from CNB, in particular, the impact of the needle size on the accuracy of several prognostic factors. Therefore, the aim of

For reprints and all correspondence: Takuya Moriya, Department of Pathology, Tohoku University Hospital. 1-1 Seiryo-machi, Aoba-ku, Sendai 980-8574, Japan. E-mail: moriya@patholo2.med.tohoku.ac.jp

this study is to evaluate the reliability of the information obtained from CNB with respect to certain histopathological factors as well as those influenced by needle thickness.

## PATIENTS AND METHODS

We studied 111 women (112 lesions) with breast cancer whose ages ranged from 29 to 80 years (mean: 55.3 years). Between January 2000 and May 2005, they underwent CNB and subsequent surgical excision at Tohoku University Hospital. Patients who received neo-adjuvant therapy or radiotherapy during the period between the CNB and the surgical excision were excluded. All the core biopsies were performed under image guidance. Ultrasound guidance using a 16-gauge true-cut needle with an automated biopsy device was employed in 91 cases (81%), while stereotactic guidance using an 11-gauge vacuum-assisted biopsy device was employed in 21 cases (19%), which demonstrated only calcification upon mammography. The number of cores ranged from 1 (88 cases) to 2 (3 cases) when the 16-gauge needle was used and ranged from 1 to 17 with a mean value of 7.7 when the 11-gauge needle was used.

Therapeutic excision was performed in each case. Partial mastectomy was performed in 92 cases (82%) while total mastectomy was carried out in 20 cases (18%). The partial mastectomy specimen was serially sectioned into 5-mm thick slices and all the slices were processed for histological diagnosis (8). In the total mastectomy cases, an adequate number of slices were retained for diagnosis. All the specimens were fixed in 10% formalin, embedded in paraffin and sectioned into slices 2–3 μm thick; staining with hematoxylin-eosin (HE) and immunohistochemicals was then performed. For determining the hormone receptor status, we employed the avidin-streptavidin immunoperoxidase method using the clone 6F11 antibody (Ventana) for ER and the clone 6 antibody (Ventana) for PR in an automated immunostainer (Benchmark System: Ventana Medical Systems, Inc.). To evaluate the human epidermal growth factor receptor-2 (HER2) status, we used a standardized immunohistochemistry kit (HercepTest for Immunoenzymatic Staining: DAKO) (9).

Slides from both CNB and the surgery were independently reviewed in a blinded fashion by two pathologists. The following six factors were considered: histological type, nuclear grade (pleomorphism), histological grade, ER status, PR status and HER2 status. In cases of inter-observer disagreement, a conclusion was reached after sufficient discussion.

Assignment of the histological type was based on the WHO classification from 2003 (10). When we could only observe a malignant (ductal) cell cluster without a border in the stroma in the CNB slides, we diagnosed only 'ductal carcinoma' (in which the invasive component of the tumor could not be determined). The histological grade was assigned using the Nottingham grading system (11). The nuclear grade was evaluated based on three tiers, namely, grades 1 (mild), 2 (intermediate) and 3 (severe), according to the same WHO classification system. The ER and PR results were assessed semi-quantitatively using Allred's scoring system (12). The results were categorized as positive when the total score (TS), expressed as the sum of the proportion score (PS) and the intensity score (IS), was more than two. With regard to HER2, membranous staining was graded as negative (score 0 or 1+), weakly positive (score 2+) and strongly positive (score 3+).

In order to determine the impact of the needle size on diagnostic accuracy, we also analyzed the effect of the relationship between the needle size and the absolute concordance rate on the evaluation of each factor.

Agreement between the results from CNB and those from surgical excision was statistically analyzed using the absolute concordance rate and $\kappa$ statistic values. The $\chi^2$ test or Fisher's exact test was used to examine the association of the needle size and the absolute concordance rate. The Cochran–Cox method was used for evaluating the relationship between the size of invasion and the accuracy of the estimation of the invasion. In this study, $P$ values less than 0.05 were considered significant.

## RESULTS

### Histological Type

All the cases that were diagnosed to be malignant on CNB proved to be breast cancer upon subsequent surgical excision (positive predictive value = 100%). In the final (excisional) diagnosis, there were 70 (62%) cases of invasive ductal carcinoma not otherwise specified (IDC), 30 (27%) cases of non-invasive ductal carcinoma (DCIS), seven (6%) cases of invasive lobular carcinoma (ILC), three (3%) cases of mucinous carcinoma, and one case each of apocrine carcinoma and tubular carcinoma (Table 1). The histological type on CNB correlated exactly (including the distinction between *in situ* and invasive carcinomas, and ductal and specific type carcinomas, i.e. lobular, mucinous and apocrine carcinomas) with that of the excisional specimen in 87 of 105 (83%) cases, except in seven cases in which the invasive component of the tumor could not be determined.

All 60 cases diagnosed as invasive carcinoma at CNB were also invasive carcinoma at excision. Of the 45 cases of *in situ* lesions diagnosed with CNB, 29 (64%) showed non-invasive ductal carcinoma at surgical excision. At CNB, 16 of the 45 (36%) *in situ* lesions were found to have invasive carcinoma at surgical excision.

The characteristics of these 16 cases were as follows. The mean size of invasive carcinoma was 8.8 mm (1–19 mm). The size (8.8 mm) was significantly smaller ($P < 0.05$) than that of the invasive carcinoma (2–80 mm, mean: 17.6 mm) diagnosed both at CNB and at surgical excision (histological type concordant cases). In 11 (69%) of these cases, the size was equal to or less than 4 mm. The mean number of invasive sites was 6.8 (1–16). Eleven (69%) cases had multiple

**Table 1.** Comparison of histological type in CNB and surgical excision

| CNB | Surgical excision | | | | | |
|---|---|---|---|---|---|---|
| | IDC | DCIS | ILC | Muc | Apo | Tub |
| IDC | **50** | 0 | 1 | 0 | 0 | 1 |
| DCIS | 14 | **29** | 0 | 0 | 1 | 0 |
| DC | 6 | 1 | 0 | 0 | 0 | 0 |
| ILC | 0 | 0 | **5** | 0 | 0 | 0 |
| Muc | 0 | 0 | 0 | **3** | 0 | 0 |
| LCIS | 0 | 0 | 1 | 0 | 0 | 0 |
| | 70 | 30 | 7 | 3 | 1 | 1 |
| | 62% | 27% | 6% | 3% | 1% | 1% |

IDC, invasive ductal carcinoma; ILC, invasive lobular carcinoma; DCIS, ductal carcinoma *in situ*; DC, ductal carcinoma in which invasion could not be determined; LCIS, lobular carcinoma *in situ*; Muc, mucinous carcinoma; Tub, tubular carcinoma.

invasion sites. All 16 cases presented comedonecrosis in *in situ* carcinoma and the nuclear grade was intermediate or high in surgical excision specimens. Further, it should be noted that four cases had metastasis to the axillary lymph node.

### Nuclear Grade (Pleomorphism)

Among 112 patients, with respect to the nuclear grade, the concordance between the results of CNB and those of surgical excision in 68 cases was 61% with a κ statistic value of 0.26 (Table 2). The remaining 44 cases (39%) were discordant: 33 cases were underestimation at CNB (1-grade discordant: 31 cases, 2-grade discordant: 2 cases), while 11 cases were overestimation at CNB (all cases were 1-grade discordant).

### Histological Grade

The histological grade was evaluated in 60 cases that were identified as invasive carcinoma by both CNB and subsequent surgical excision. There was 75% (45 of 60 cases) agreement (Table 2) with a κ statistic value of 0.55. Based on the results of nuclear grade concordance, in 11 of the 15 discordant cases, the grade at CNB was lower, while in four cases, the grade at CNB was higher than that in subsequent surgical excision. However, every disagreement case was 1-grade discordant.

### Estrogen Receptor and Progesterone Receptor

At surgical excision, ER was expressed in 80% (90/112) of the cases, while PR was expressed in 76% (85/112) of the cases (Table 3). The absolute concordance rate between the CNB and the surgical specimen was 95% (106/112) in ER and 88% (99/112) in PR. When the ER/PR status of the excisional specimen was regarded as the golden standard, the sensitivity, specificity and positive predictive values of CNB were 96, 91 and 98% in ER and 89, 85 and 95% in PR, respectively.

If cases in which at least one of the hormone receptors (ER or PR) was positive were defined as hormone receptor-positive cases, the number of discordant cases was seven (6%). Among these, four cases were negative at CNB but positive at excision. Three cases were positive at CNB but negative at excision. There was 94% concordance with a κ statistic value of 0.79. The sensitivity, specificity and positive predictive values at CNB were 96, 85 and 97%, respectively.

### HER2

HER2 was also evaluated in 60 cases. In 13 (22%) of the 60 cases, HER2 was expressed in the excisional specimen. There was 88% (53 of 60 cases) agreement with a κ statistic value of 0.65. The sensitivity, specificity and positive predictive values of CNB were 69, 94 and 75%, respectively (Table 4). In cases where the score was 3+ (strongly positive) at either CNB or surgical excision, all six cases showed concordance between the results from CNB and those from the surgical specimen with respect to discrimination between positive and negative cases.

**Table 2.** Comparison of the nuclear grade (pleomorphism) and the histological grade in CNB and surgical excision

| CNB | Nuclear grade: surgical excision | | | | CNB | Histological grade: surgical excision | | | |
|---|---|---|---|---|---|---|---|---|---|
| | 1 | 2 | 3 | | | I | II | III | |
| 1 | **3** | 15 | 2 | 20 (18%) | I | **11** | 4 | 0 | 15 (25%) |
| 2 | 5 | **50** | 16 | 71 (63%) | II | 2 | **29** | 7 | 38 (63%) |
| 3 | 0 | 6 | **15** | 21 (19%) | III | 0 | 2 | **5** | 7 (12%) |
| | 8 (7%) | 71 (63%) | 33 (30%) | **112** | | 13 (22%) | 35 (58%) | 12 (20%) | **60** |

Absolute concordance rate, **61%** (68/112); kappa statistic value, **0.26.**

Absolute concordance rate, **75%** (45/60); kappa statistic value, **0.55.**

**Table 3.** Comparison of ER and PR and surgical excision

| CNB | ER: surgical excision | | | CNB | PR: surgical excision | | |
|---|---|---|---|---|---|---|---|
| | Positive | Negative | | | Positive | Negative | |
| Positive | **86** | 2 | 88 (79%) | Positive | **76** | 4 | 80 (71%) |
| Negative | 4 | **20** | 24 (21%) | Negative | 9 | **23** | 32 (29%) |
| | 90 (80%) | 22 (20%) | **112** | | 85 (76%) | 27 (24%) | **112** |

Absolute concordance rate, **95%** (106/112); kappa statistic value, **0.84.**

Absolute concordance rate, **88%** (99/112); kappa statistic value, **0.70.**

### Impact of the Needle Size

Table 5 shows the impact of the needle size on several prognostic factors. With respect to the evaluation of the nuclear and histological grades, in comparison with the 16-gauge core, the 11-gauge core showed a more marked trend toward greater accuracy; however, all the factors analyzed in this study did not reach statistical significance ($P = 0.17–0.96$).

## DISCUSSION

CNB may be a good diagnostic procedure for distinguishing between *in situ* and invasive carcinoma, and this is a great advantage that CNB has over FNA. In addition, more information can be obtained by immunohistochemical analysis of the CNB specimen. However, underestimation of the invasion is an unavoidable problem in CNB because the quantity of the specimen is limited. Several reports have documented this (13–15). The incidence of underestimation has been reported to be 19–35% using the 14-gauge core, approximately 10% using the 11-gauge vacuum-assisted core and 4% using the 8-gauge vacuum-assisted core.

In comparison with the results of earlier studies, our results show a higher rate (11-gauge vacuum-assisted core: 25%, 16-gauge core: 41%) of underestimation of invasion. Unlike previously published studies, in this study, we performed minute pathological examination (the entire specimen was serially sectioned into 5-mm thick slices). This would explain the higher underestimation of the invasion rate. The diagnosis of *in situ* carcinoma is influenced to a great extent by the degree of pathological examination. The rate may become higher if even thinner slices are examined.

Therefore, when dealing with a case of *in situ* carcinoma diagnosed at CNB, we should consider the nuclear grade and comedonecrosis, and the diagnosis should be comprehensive, involving the use of various types of imaging techniques (mammography, ultrasonography (US), computed tomography (CT) and magnetic resonance imaging (MRI). Additionally, in this present series, there were four cases with axillary lymph node involvement. This shows that it is necessary to perform sentinel lymph node biopsy or lymph node dissection in some cases, even if the diagnosis at CNB is DCIS.

Information on the histological type is important in cases of invasive breast carcinomas. In 60 cases of invasive carcinoma that were diagnosed by CNB, our results showed excellent agreement (97%, 58 of 60 cases) with regard to the histological type even when the special types of carcinoma were included. In the case of invasive carcinomas, a 16-gauge core was sufficient to estimate the histological type. A recent study indicated (16) that the discordance was due to the inclusion of special types and variants of invasive carcinomas. In this series, since there were few incidences of special types of carcinomas and all of these showed typical histological findings, our results may not have been influenced by minor variations. In this study, we evaluated the nuclear and histological grades of specimens taken at CNB and compared these with those of specimens taken at

**Table 4.** Comparison of HER2 in CNB and surgical excision

| CNB | HER2: surgical excision | | |
|---|---|---|---|
| | Positive | Negative | |
| Positive | **9** | 3 | 12 (20%) |
| Negative | 4 | **44** | 48 (80%) |
| | 13 (22%) | 47 (78%) | **60** |

Absolute concordance rate, **88%** (53/60); kappa statistic value, **0.65.**
HER2 positive: score 3+, 2+; negative: score 1+, 0 in the Hercep Test.

**Table 5.** Impact of the needle size on prognostic factors

| | 11G | | 16G | | *P* value |
|---|---|---|---|---|---|
| | κ | ACR (%) | κ | ACR (%) | |
| Nuclear grade | 0.57 | 76 | 0.18 | 57 | 0.17 |
| Histological grade | 1.00 | 100 | 0.45 | 70 | 0.47 |
| ER | 0.69 | 90 | 0.87 | 96 | 0.69 |
| PR | 0.86 | 95 | 0.67 | 87 | 0.48 |
| HER2 | – | 100 | 0.58 | 86 | 0.96 |

ACR, absolute concordance rate; κ, kappa statistic value.

surgical excision. In particular, the histological grade is a powerful prognostic factor of invasive breast carcinoma. There are 61% cases with a fair κ value (0.26) and 75% cases with a moderate κ value (0.55). These results are similar to those reported previously (59–75%) (16–20).

In the discordant cases, the grade at CNB tended to be lower than that at surgical excision. Previous studies noted that this tendency of the histological grade was due to underestimation of the mitotic count at CNB. In this study, underestimation of the nuclear grade (pleomorphism) is not negligible. Similar results were reported in previous studies (17–19), but the reasons were not described in detail. In the present study, we also analyzed the impact of the needle size on the nuclear grade. The κ statistic value was calculated to be 0.57 using an 11-gauge core and 0.18 using a 16-gauge core. This result indicates that the nuclear grade predicted using the 11-gauge core tended to be more accurate than that obtained with the 16-gauge core, although a significant difference was not found between the two needle sizes. One plausible explanation for this observation is that a stronger experimental artifact, resulting from the crushing of specimens, occurs when the samples are obtained by the 16-gauge core than when they are removed by the 11-gauge vacuum-assisted biopsy device.

The hormone receptor status is also a very important and independent prognostic factor in breast cancer. In our study, hormone receptors were accurately evaluated at CNB. An almost perfect κ value (0.84) in ER and a substantial κ value (0.70) in PR were observed. The concordance of PR was lower than that of ER. This can be associated with the lower incidence of PR-expressing cells in the whole tumor because the Allred total score of PR (mean: 4.5) was lower than that of ER (mean: 5.6). In general, if the result of ER 'and/or' PR is positive, endocrine therapy is indicated. Based on this observation, an extremely high concordance (94%) was observed in this study, while the needle size had no influence. If we use a 16-gauge needle, the core could be reliably used for the assessment of the hormone receptor status.

Although the immunohistochemical staining results for ER/PR at CNB may be reliable for determining therapeutic indications, seven discordant cases (6%) were observed. There were four cases that were CNB-negative and excision-positive and three cases that were of the opposite type. The characteristics of the former cases are mainly due to intratumoral heterogeneity. In the latter cases, only the area of the CNB specimen was positive and some investigators (21–22) have noted that such situations could exist because of more rapid and constant fixation. Douglas-Jones et al. (23) suggested that ER expression was higher in the CNB than in the excised tumors. ER expression was higher at the periphery of tumors than at the center. The higher ER expression in CNB might reflect the greater possibility of the peripheral part of a tumor being sampled when CNB is performed. As long as these cases exist, routine immunostaining of specimens at CNB will have great significance in determining the indications of endocrine therapy. Especially when we determine post-operative systemic therapy in the cases given neo-adjuvant therapy, the results determined by the specimens from core needle biopsy will be more important than those from surgery, which are denatured by pre-operative therapy. With regard to the HER2 status, the diagnostic accuracy (particularly the sensitivity) of CNB was relatively low when compared to that of the hormone receptor status. Conversely, CNB demonstrated excellent sensitivity in cases where the score was 3+. This result is clinically useful in metastatic or inoperable patients. In contrast, cases with a score of 2+ or 1+ should be regarded as indeterminate.

In summary, the underestimation rate for detecting invasion was higher in this study than in previous reports; this is probably due to more precise examination of the excised specimen. Even if a thicker core is used, the problems cannot be completely resolved. If invasive components are detected among the CNB specimens, they can provide reliable information on the histological type, in spite of the use of a thin (16-gauge) needle. The accuracy with which the nuclear/histological grade is estimated is modest and it may be improved by optimizing the needle size and/or noting the nuclear/histological characteristics of the CNB specimen. Hormone receptor evaluation is accurate, even when the single 16-gauge core is used. Determination of the HER2 status in CNB was reliable only in cases where the score was 3+. In order to obtain information on the characteristics of the target lesions, it is necessary to choose a needle of appropriate size. Although CNB has performance limitations, it can provide reliable prognostic factors. It would be worthwhile using the information obtained from CNB in clinical practice.

## Acknowledgments

We would like to express our gratitude to the staff at the Department of Pathology and Surgical Oncology for technical assistance and collection of the tissues.

**Conflict of interest statement**

None declared.

## References

1. Elvecrog EL, Lechner MC, Nelson MT. Nonpalpable breast lesions. Correlation of stereotaxic large-core needle biopsy and surgical biopsy results. *Radiol* 1993;188:453–55.
2. Parker SH, Burbank F, Jackman RJ, Aucreman CJ, Cardenosa G, Cink TM, et al. Percutaneous large-core breast biopsy. A multi-institutional study. *Radiol* 1994;193:359–64.
3. Nguyen M, McCombs MM, Ghandehari S, Kim A, Wang H, Barsky SH, et al. An update on core needle biopsy for radiologically detected breast lesions. *Cancer* 1996;78:2340–5.
4. Fajardo LL, Pisano ED, Caudry DJ, Gatsonis CA, Berg WA, Connolly J, et al. Stereotactic and sonographic large-core biopsy of nonpalpable breast lesions. Results of the Radiologic Diagnostic Oncology Group V study. *Acad Radiol* 2004;11:293–308.
5. Brenner RJ, Bassett LW, Fajardo LL, Dershaw DD, Evans WP, III, Hunt R, et al. Stereotactic core-needle breast biopsy: a multi-institutional prospective trial. *Radiol* 2001;218:866–72.

6. Verkooijen HM, and Core Biopsy After Radiological Localisation (COBRA) Study Group. Diagnostic accuracy of stereotactic large-core needle biopsy for nonpalpable breast disease. Results of a multicenter prospective study with 95% surgical confirmation. *Int J Cancer* 2002;99:853–9.
7. Lower EE, Glass EL, Bradley DA, Blau R, Heffelfinger S. Impact of metastatic estrogen receptor and progesterone receptor status on survival. *Breast Cancer Res Treat* 2005;90:65–70.
8. Yang M, Moriya T, Oguma M, De La Cruz C, Endoh M, Ishida T, et al. Microinvasive ductal carcinoma (T1mic) of the breast. The clinicopathological profile and immunohistochemical features of 28 cases. *Pathol Int* 2003;53:422–8.
9. Birner P, Oberhuber G, Stani J, Reithofer C, Samonigg H, Hausmaninger H, et al. Austrian Breast & Colorectal Cancer Study Group. Evaluation of the United States Food and Drug Administration-approved scoring and test system of HER-2 protein expression in breast cancer. *Clin Cancer Res* 2001;7:1669–75.
10. Tavassoli FA, Devilee P, editors. World Health Organization Classification of tumours. Pathology and genetics of tumours of the breast and female genital organs. Lyon: IARC Press 2003, 9–112.
11. Elston CW, Ellis IO. Pathological prognostic factors in breast cancer. I. The value of histological grade in breast cancer: experience from a large study with long-term follow-up. *Histopathology* 1991;19:403–10.
12. Allred DC, Harvey JM, Berardo M, Clark GM. Prognostic and predictive factors in breast cancer by immunohistochemical analysis. *Mod Pathol* 1998;11:155–68.
13. Nath ME, Robinson TM, Tobon H, Chough DM, Sumkin JH. Automated large-core needle biopsy of surgically removed breast lesions: comparison of samples obtained with 14-, 16-, and 18-gauge needles. *Radiol* 1995;197:739–42.
14. Brem RF, Schoonjans JM, Goodman SN, Nolten A, Askin FB, Gatewood OM. Nonpalpable breast cancer: percutaneous diagnosis with 11- and 8-gauge stereotactic vacuum-assisted biopsy devices. *Radiol* 2001;219:793–96.
15. Brem RF, Schoonjans JM, Sanow L, Gatewood OM. Reliability of histologic diagnosis of breast cancer with stereotactic vacuum-assisted biopsy. *Am Surg* 2001;67:388–92.
16. Andrade VP, Gobbi H. Accuracy of typing and grading invasive mammary carcinomas on core needle biopsy compared with the excisional specimen. *Virchows Arch* 2004;445:597–602.
17. Sharifi S, Peterson MK, Baum JK, Raza S, Schnitt SJ. Assessment of pathologic prognostic factors in breast core needle biopsies. *Mod Pathol* 1999;12:941–5.
18. Harris GC, Denley HE, Pinder SE, Lee AH, Ellis IO, Elston CW, et al. Correlation of histologic prognostic factors in core biopsies and therapeutic excisions of invasive breast carcinoma. *Am J Surg Pathol* 2003;27:11–15.
19. Monticciolo DL. Histologic grading at breast core needle biopsy: comparison with results from the excised breast specimen. *Breast J* 2005;1:9–14.
20. Badoual C, Maruani A, Ghorra C, Lebas P, Avigdor S, Michenet P. Pathological prognostic factors of invasive breast carcinoma in ultrasound-guided large core biopsies. A correlation with subsequent surgical excisions. *Breast* 2005;14:22–7.
21. Zidan A, Christie Brown JS, Peston D, Shousha S. Oestrogen and progesterone receptor assessment in core biopsy specimens of breast carcinoma. *J Clin Pathol* 1997;50:27–9.
22. Connor CS, Tawfik OW, Joyce AJ, Davis MK, Mayo MS, Jewell WR. A comparison of prognostic tumor markers obtained on image-guided breast biopsies and final surgical specimens. *Am J Surg* 2002;184:322–4.
23. Douglas-Jones AG, Collett N, Morgan JM, Jasani B. Comparison of core oestrogen receptor (ER) assay with excised tumour: intratumoral distribution of ER in breast carcinoma. *J Clin Pathol* 2001;54:951–5.

# Promoter methylation status of the Cyclin D2 gene is associated with poor prognosis in human epithelial ovarian cancer

Michiko Sakuma,[1,3] Jun-ichi Akahira,[2] Kiyoshi Ito,[1] Hitoshi Niikura,[1] Takuya Moriya,[2] Kunihiro Okamura,[1] Hironobu Sasano[2] and Nobuo Yaegashi[1]

Departments of [1]Obstetrics and Gynecology, and [2]Pathology Tohoku University, Graduate School of Medicine, 1-1 Seiryo-machi, Aoba-ku Sendai, 980-8574 Japan

(Received March 18, 2006/Revised July 28, 2006/2nd Revised November 10, 2006/Accepted November 18, 2006/Online publication January 15, 2007)

**Gene silencing associated with aberrant DNA methylation of promoter CpG islands is one mechanism through which several genes may be inactivated in human cancers. Cyclin D2, a member of the D-type cyclins, implicated in cell cycle regulation, differentiation and malignant transformation, is inactivated due to aberrant DNA methylation in several human cancers. In the present study, we examined the promoter methylation status and expression of Cyclin D2 in human epithelial ovarian cancer, and then determined the relationship between methylation status and various clinicopathological variables. Twelve ovarian cancer cell lines and 71 surgical specimens were examined by methylation-specific polymerase chain reaction and quantitative reverse transcription–polymerase chain reaction to evaluate the methylation status and expression of the Cyclin D2 gene. The relationship between methylation status and various clinicopathological variables was evaluated using statistical analysis. Aberrant methylation of Cyclin D2 was present in five of 12 ovarian cancer cell lines and 16 of 71 primary ovarian cancer tissues. In five cell lines with methylation, expression of the Cyclin D2 gene tended to be lower than in cell lines without methylation. In ovarian cancer tissues, methylation bands were detected in 16 of 71 cases. The methylation status of Cyclin D2 was associated with advanced stage and a residual tumor size (>2 cm) ($P = 0.027$ and $P = 0.031$, respectively). Based on univariate analysis, patients with aberrant methylation of the Cyclin D2 promoter had a significantly worse chance of disease-free survival than those without methylation ($P = 0.021$). Our results suggest that aberrant promoter methylation of the Cyclin D2 gene is significantly associated with patient prognosis in epithelial ovarian cancer. (*Cancer Sci* 2007; 98: 380–386)**

Epithelial ovarian cancer is the most common and deadliest gynecological malignancy in developed countries. Early stages of ovarian cancer are generally asymptomatic and difficult to detect. By the time clinical diagnosis is made, most patients have widespread tumor dissemination.[1] Despite a high response rate to first-line chemotherapy, the prognosis of these women is poor, with an overall 5-year survival rate of only 10–20%.[1,2]

Epigenetic alterations, changes that affect gene expression but not the gene sequence itself, are believed to be one mechanism by which tumor suppressor genes are inactivated in human cancers.[3,4] In particular, hypermethylation of cytosine residues in CpG islands leads to heritable gene silencing via the formation of a repressive chromatin structure.[5,6] Studies of DNA hypermethylation in human ovarian cancer have identified some key genes as targets for epigenetic downregulation, including some hormone receptors,[7] cytokines, cell signaling intermediates, adhesion molecules,[8] DNA damage checkpoint genes,[9] and regulators of the cell cycle.[10] The cell cycle regulators, notably the cyclins, have the potential to function as oncogenes when regulated inappropriately.

The cyclins are a family of proteins that dictate transitions between phases of the cell cycle by regulating the activity of their downstream effectors, the cyclin-dependant kinases (cdk). The D-type cyclins, D1, D2 and D3, play a critical role in early checkpoint regulation of the $G_1$ phase of the cell cycle. They activate cdk4 and cdk6, leading to the phosphorylation of the retinoblastoma tumor suppressor protein (Rb). This, in turn, dissociates Rb from the transcription factor E2F, thereby permitting DNA transcription. Given the critical role of the D-type cyclins in cell cycle regulation, their abnormal or untimely expression could disrupt the normal cell cycle, resulting in cell proliferation.[11] In fact, Cyclin D1 is considered by some to be a putative protooncogene, as it is overexpressed in a number of tumor types, including breast cancer, thyroid carcinoma, stomach cancer and lymphomas.[12] Aberrant expression of Cyclin D2 has also been demonstrated in human ovarian granulose cell tumors and testicular germ cell tumor cell lines.[13]

Although well known for their proliferation-promoting activity, the D-type cyclins (notably D2) also have growth-inhibitory effects. Cyclin D2 has been shown to be dramatically upregulated under conditions of growth arrest in human and murine fibroblasts. Furthermore, transient overexpression of Cyclin D2 efficiently inhibits cell cycle progression and DNA synthesis. This suggests that an alternative role for Cyclin D2 may be to promote exiting from the cell cycle and maintenance of a nonproliferative state.[14] The expression of Cyclin D2 is frequently lost in human breast cancers, gastric cancers, lung cancers and ovarian granulose cell tumors. This loss of expression is the result of promoter hypermethylation.[10,15–18]

In the present study, we examined the promoter methylation status and gene expression of Cyclin D2 in human epithelial ovarian cancer cell lines. We also evaluated the correlation between methylation status of the Cyclin D2 promoter and various clinicopathological parameters in patients with epithelial ovarian cancer.

## Materials and Methods

**Cell lines.** Twelve ovarian carcinoma cell lines were used. OVCAR3, SKOV3 (both adenoarcinomas), Caov3, OV90 (both serous adenocarcinoma), TOV21G, ES2 (both clear cell adenocarcinoma) and TOV112D (endometrioid adenocarcinoma) were purchased from American Type Culture Collection. JHOS2, JHOS3, HTOA (all serous adenocarcinoma), OMC3 (mucinous adenocarcinoma) and JHOC5 (clear cell adenocarcinoma) were purchased from Riken Cell Bank (Tsukuba). Cell lines were maintained in DMEM/F12 medium (Invitrogen), supplemented

[3]To whom correspondence should be addressed.
E-mail: msakuma@mail.tains.tohoku.ac.jp



doi: 10.1111/j.1349-7006.2007.00394.x

with 10% fetal bovine serum and 1% penicillin/streptomycin (Invitrogen), and incubated in a 5% $CO_2$ atmosphere at 37°C.

**Surgical specimens and clinical data.** The research protocol was approved by the Ethics Committee of Tohoku University Graduate School of Medicine, Sendai, Japan. We examined 71 ovarian cancer specimens obtained from patients treated between 1988 and 2002 at Tohoku University Hospital, Sendai, Japan. All specimens were retrieved from the surgical pathology files at Tohoku University Hospital. Informed consent was obtained from each patient. Specimens were fixed in 10% formalin and embedded in paraffin. Patient age, performance status on admission, histology, stage, grade, residual tumor after primary surgery, and overall survival were obtained from a chart review. The median follow-up time for patients was 59 months (range, 4–120 months). Performance status was defined according to the WHO criteria.[19] Histology, stage and grading followed the FigO criteria.[20] Residual tumor was defined as the amount of unresectable tumor left following primary volume reductive surgery. Optimal volume reduction was achieved when the residual tumor was less than 2 cm. Patients with a residual tumor greater than 2 cm were considered to have suboptimal volume reduction. Overall survival was calculated from the time of initial surgery to death or the date of the last contact. Survival times of patients still alive or lost to follow-up were censored as of December 2002.

An ovarian tissue obtained from a 50-year-old woman who had received surgical treatment for benign uterine tumor was used as a normal ovarian tissue for methylation-specific polymerase chain reaction (MSP) and reverse transcription–polymerase chain reaction (RT-PCR).

**Methylation-specific polymerase chain reaction.** The methylation status of the samples was assessed using MSP as described previously.[21] Genomic DNA from ovarian cancer cell lines was extracted using the AquaPure Genomic DNA kit (Bio-Rad). Genomic DNA from ovarian tumor specimens was extracted from paraffin blocks. For each tissue, the presence of carcinoma was confirmed on a H&E stained section. For DNA extraction, three 5-μm tissue sections from the same block were scraped from the slide and treated with Dexpat (Takara). The quality and integrity of the DNA were evaluated in terms of the $A_{260/280}$ ratio. Genomic DNA (1 μg) was treated with sodium bisulfite using a CpGenome DNA modification kit (Intergen) according to the manufacturer's protocol. Amplification was conducted in a 20-μL reaction volume containing 2 μL of 10× ExTaq buffer, 1.5 μL of 2.5 mM $MgCl_2$, 1 mM of each primer, 1.5 mL of 2.5 mM dNTPs, and 1 unit of Takara ExTaq polymerase (Takara). The reaction was cycled for 40 cycles, each of which consisted of denaturation at 95°C for 30 s, annealing at 56°C for 30 s, and extension at 72°C for 45 s, followed by a 7-min extension at 72°C. The primers used were 5′-AGAGTATGTGTTAGGGTTGATT-3′ and 5′-ACATCCTCACCAACCCTCCA-3′ (−1431 to −1326, 106-bp) for the unmethylated reaction (U), and 5′-GGCGGATTTTATCGTAGTCG-3′ and 5′-CTCCACGCTCGATCCTTCG-3′ (−1404 to −1304, 101-bp) for the methylated reaction (M).[18] Universal unmethylated human genomic DNA (Intergen) was used as a positive control for the unmethylated reaction. Universal methylated human male genomic DNA (Intergen) was used as a positive control for the methylated reaction. Reaction products were separated by electrophoresis on 3% agarose gel, stained with ethidium bromide, and visualized under ultraviolet light.

**Quantitative RT-PCR.** Total RNA was isolated from cells by phenol–chloroform extraction using Isogen reagent (Nippon Gene). RNA was treated with RNase-free DNase (Roche Diagnostics; 1 μg/μL) for 2 h at 37°C, followed by heat inactivation at 65°C for 10 min. Total RNA (5 μg) was reversed transcribed using the Superscript II first-strand synthesis system (Invitrogen) with random hexamers according to the manufacturer's protocol. Quantitative polymerase chain reaction (PCR) was carried out using an iCycler system (Bio-Rad). For the determination of Cyclin D2 cDNA content, a 25-μL reaction mixture consisting of 23 μL iQSYBR Green MasterMix, 1 μL of each primer and 1 μL of cDNA template was cycled as follows: 2-min denaturation at 90°C, 30-s annealing at either 60°C (for Cyclin D2) or 62°C (for β-actin), and 1.5-min extension at 72°C. Primers for PCR reactions were as follows: Cyclin D2-F, 5′-TACTTCAAGTGCGTGCAGAAGGAC-3′ and Cyclin D2-R, 5′-TCCCACACTTCCAGTTGCGATCAT-3′;[22] and β-actin-F, 5′-CCAACCGCGAGAAGATGAC-3′ and β-actin-R, 5′-GGAAGGAAGGCTGGAAGAGT-3′.[23] β-Actin primers were utilized as an internal positive control and Cyclin D2 expression level was calculated by dividing the quantity obtained for Cyclin D2 by the quantity obtained for β-actin. Two independent RT-PCR reactions were carried out for each sample.

**5-Aza-2′-deoxycitidine and trichostatin A treatment.** To confirm that epigenetic change contributed to loss of Cyclin D2 gene expression, we assessed the effect of 5-aza-2′-deoxycitidine (5azaC) (Sigma), a demethylating agent, and trichostatin A (TSA) (Sigma), a histone deacetylase inhibitor, on Cyclin D2 mRNA expression and cell growth of ovarian cancer cell lines by quantitative RT-PCR and cell count, respectively.

Ovarian cancer cell lines (OMC3, OVCAR3, JHOS2, JHOC5 and SKOV3) were cultured at a point of 70% confluence in 10-cm cell dishes. They were treated with 1.0 μM 5azaC for 3 or 5 days. They were also treated with 0.5 μM TSA.[24,25] We set up TSA treatment times of 4, 8, 16 and 32 h, and the treatments for 8 and 16 h appeared the most effective for gene expression compared to control culture (data not shown). Total RNA was prepared at each time point and the expression of Cyclin D2 mRNA was analyzed by quantitative RT-PCR. Furthermore, we investigated the effects of these chemical agents on cell growth of ovarian cancer cell lines by cell count at each time point.

**Immunohistochemistry.** For the purpose of investigating cell proliferation we examined the immunohistochemical expression of Ki-67 in ovarian cancer tissue. Immunohistchemical analysis was carried out with the streptavidin–biotin amplification method using the NX/ES IHC system (Ventana Medical Systems). Monoclonal antibody for Ki-67 (MIB-1) was purchased from DAKO. For antigen retrieval, the slides ware heated in an autoclave at 120°C for 5 min in citric acid buffer (2 mM citric acid and 9 mM trisodium citrate dyhydrate [pH 6.0]). The dilution of primary antibody was 1:50. Scoring of Ki-67 in carcinoma cells was counted independently by two of the authors (M. S. and J. A.), and the percentage of immnunoreactivity in at least 500 carcinoma cells (i.e. the labeling index) was determined.

**Statistical analysis.** Statistical analysis was carried out using Stat View 5.0 software (SAS Institute). The correlation between the Cyclin D2 mRNA expression level and methylation status was assessed using the Mann–Whitney *U*-test. The statistical significance between methylation status and various clinicopathological parameters was evaluated using Friedman's $\chi^2$ *r*-test and the Mann–Whitney *U*-test. A univariate analysis of prognostic significance for prognostic factors was carried out using the log-rank test after each survival curve was obtained by the Kaplan–Meier method. Multivariate analysis was carried out using the Cox regression model to evaluate the predictive power of each variable independently. All patients who could be assessed were included in the intention-to-treat analysis. A result was considered significant when the *P*-value was less than 0.05.

## Results

**Methylation status of the Cyclin D2 gene in ovarian cancer cell lines and tissues.** Bands corresponding to methylated Cyclin D2 were

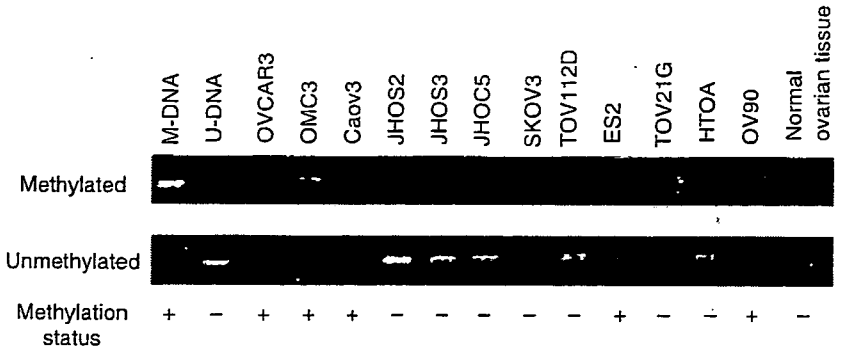


**Fig. 1.** Methylation status of the Cyclin D2 gene in ovarian cancer cell lines and a normal ovarian tissue. The 101-bp bands in the 'Methylated' lanes indicate the presence of methylated alleles of the Cyclin D2 gene. The 106-bp bands in the 'Unmethylated' lanes correspond to the unmethylated alleles. Methylation status is denoted as follows: +, methylated alleles with or without unmethylated alleles; −, purely unmethylated alleles. M-DNA, universal methylated human male genomic DNA, was used for positive control of methylated reaction. U-DNA, universal unmethylated fetal genomic DNA, was used for positive control of unmethylated reaction.

**Table 1. Patient characteristics and cyclin D2 methylation status**

| Variable | *n* | Cyclin D2 methylation | | | *P*-value |
|---|---|---|---|---|---|
| | | + | − | % | |
| Age (years) | | | | | |
| <50 | 29 | 8 | 21 | 27.6 | |
| ≥50 | 42 | 8 | 34 | 19 | NS |
| Performance status† | | | | | |
| 0–1 | 51 | 9 | 42 | 17.6 | |
| 2–4 | 19 | 7 | 12 | 36.8 | NS |
| FigO stage | | | | | |
| I, II | 35 | 4 | 31 | 2.9 | |
| III, IV | 36 | 12 | 24 | 33.3 | 0.027 |
| Histological type of adenocarcinoma | | | | | |
| Serous | 26 | 6 | 20 | 23.1 | |
| Endometrioid | 15 | 3 | 12 | 20 | |
| Mucinous | 7 | 3 | 4 | 75 | |
| Clear cell | 23 | 4 | 19 | 17.4 | NS |
| Grade | | | | | |
| 1 | 24 | 5 | 19 | 20.8 | |
| 2 | 22 | 7 | 15 | 31.8 | |
| 3 | 17 | 3 | 14 | 17.6 | NS |
| Residual tumor size (cm) | | | | | |
| <2 | 47 | 7 | 40 | 14.9 | |
| ≥2 | 24 | 9 | 15 | 37.5 | 0.031 |
| Ki-67 labeling index (median) | | 21.6 | 23.6 | 20.4 | NS |

†0, asymptomatic and fully active; 1, symptomatic, fully ambulatory, restricted in physically strenuous activity; 2, symptomatic, ambulatory, capable of self-care, more than 50% of walking hours are spent out of bed; 3, symptomatic, limited self-care, more than 50% of time is spent in bed, but not bedridden; 4, completely disabled, no self-care, bedridden.

detected in five of 12 cell lines, three of which also contained the unmethylated band, as shown in Fig. 1. The methylated band was detected in two of five cell lines derived from serous adenocarcinoma (Caov3, OV90), in one of three cell lines from clear cell carcinoma (ES2), in the one mucinous adenocarcinoma (OMC3), but not in the endometrioid adenocarcinoma. The normal ovarian tissue was negative for the methylated band. The methylated band was detected in 16 of the 71 surgical specimens (6/26 serous, 4/23 clear cell, 3/15 endometrioid and 3/7 mucinous adenocarcinoma), as shown in Table 1.

**Expression of the Cyclin D2 gene in ovarian cancer cell lines and normal ovarian tissue.** The expression of the Cyclin D2 gene in the cell lines is presented in Fig. 2. Quantitative RT-PCR was carried out and the ratio of Cyclin D2 to β-actin was calculated to allow for comparison among the cell lines. The median value of relative Cyclin D2 gene expression in cell lines with methylation (0.015) tended to be lower than that in cell lines without methylation (0.03), although the difference was not significant ($P = 0.19$, Mann–Whitney $U$-test). The expression level of the Cyclin D2 gene in normal ovarian tissue was relatively high compared with ovarian cancer cell lines.

**Effects of 5azaC and TSA treatment on methylated cell lines.** To confirm that promoter methylation contributed to the loss of Cyclin D2 gene expression, we assessed the effect of 5azaC, a demethylating agent, on Cyclin D2 mRNA expression by quantitative RT-PCR. OMC3 and OVCAR3 cells, which were positive for the methylated band in MSP, were treated. From MSP analysis OMC3 had only methylated alleles, but OVCAR3 had both methylated and unmethylated alleles. We also assessed the effect of TSA, a histone deacetylase inhibitor, to investigate whether another epigenetic change, histone deacetylation, contributed to the silencing of Cyclin D2 gene expression. Treatment of OMC3 cells with 5azaC for 5 days led to a 2.64-fold increase in expression (Fig. 3a). Treatment of OVCAR3 cells with 5azaC for 5 days resulted in a 222-fold increase in expression (Fig. 3b). Treatment with TSA also contributed to re-expression of the Cyclin D2 gene in OMC3 and OVCAR3 cells (2.3-fold and 119-fold, respectively) (Fig. 3). These results suggested that the decreased expression of Cyclin D2 in these cell lines was related to epigenetic change, including DNA methylation or histone deacetylation.

The effects of 5azaC and TSA on cell growth are summarized in Fig. 4. Compared with cell growth in control culture, cell growth with 5azaC or TSA treatment was suppressed in each culture. These chemical agents resulted in inhibition of cell growth in these ovarian cancer cell lines simultaneous with re-expression of the Cyclin D2 gene.

**Effects of 5azaC and TSA treatment on unmethylated cell lines.** In the MSP and quantitative RT-PCR analyses, expression of the Cyclin D2 gene was decreased in some cell lines without promoter methylation. We assessed the effect of 5azaC or TSA treatment in these cell lines (JHOS2, JHOC5 and SKOV3) to investigate the participation of epigenetic change in the silencing of this gene. Treatment of JHOS2 cells with TSA resulted in higher re-expression than treatment with 5azaC (Fig. 5a). Treatment of JHOC5 cells with TSA for 16 h resulted in an 84.4-fold increase in expression, and treatment with 5azaC also led to a 137-fold increase in expression (Fig. 5b). As for SKOV3 cells, treatment with TSA did not increase the expression of this gene. These results suggest that histone deacetylation may contribute to silencing of the Cyclin D2 gene in JHOS2 and JHOC5 cells, but not in SKOV3.

**Correlation between clinicopathological parameters and methylation status of Cyclin D2 in epithelial ovarian cancer.** The clinicopathological parameters relative to the methylation status of Cyclin D2 are presented in Table 1. Methylation status was significantly associated with advanced stage and residual tumor size >2 cm.



doi: 10.1111/j.1349-7006.2007.00394.x

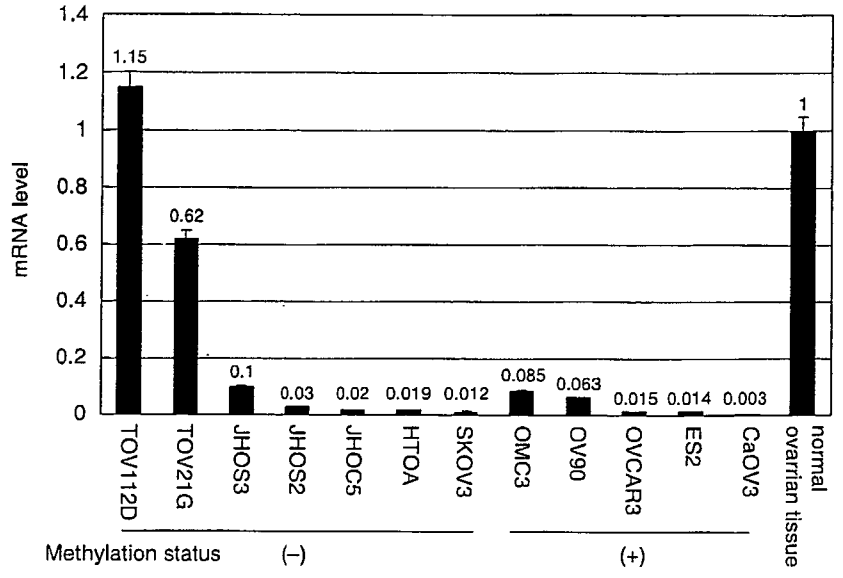


Fig. 2. Expression of the Cyclin D2 gene in ovarian cancer cell lines and normal ovarian tissue. Two independent reverse transcription–polymerase chain reactions were carried out for each sample, and the ratio of Cyclin D2: β-actin was calculated and normalized with the level of normal ovarian tissue. Methylation status is indicated in the same way as in Fig. 1.

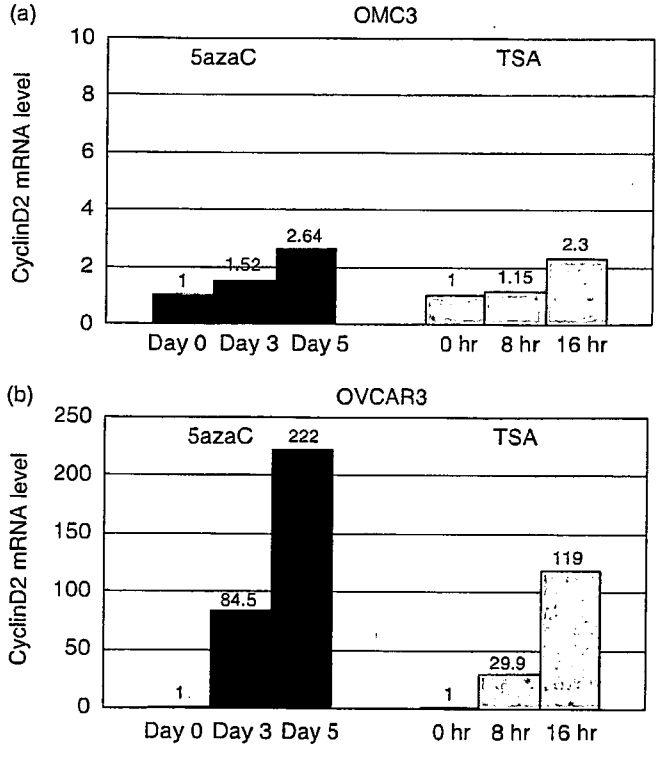


Fig. 3. Expression level of the Cyclin D2 gene as determined by quantitative reverse transcription–polymerase chain reaction in OMC3 and OVCAR3 cells following treatment with (a) 5-aza-2′-deoxycitidine (5azaC) or (b) trichostatin A (TSA). The ratio of Cyclin D2 : β-actin was calculated and normalized with the level before treatment.

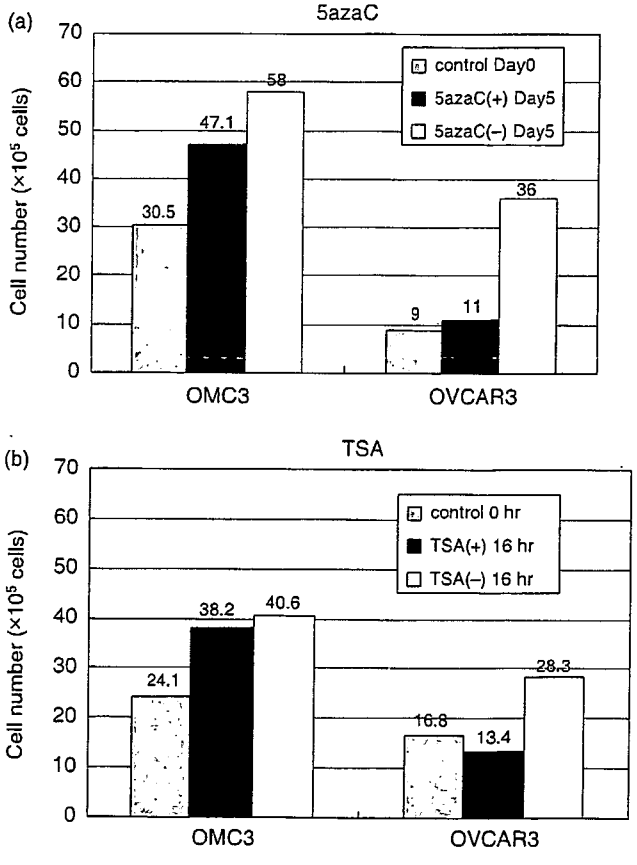


Fig. 4. Cell number of OMC and OVCAR3 cells following treatment with (a) 5-aza-2′-deoxycitidine (5azaC) or (b) trichostatin A (TSA). *Control treatment with medium alone.

There was no association between methylation status and age, performance status, histological type, histological grade or Ki-67 labeling index

The results of the univariate analysis of prognostic significance for each variable with respect to survival are summarized in Tables 2 and 3. Of the clinicopathological parameters evaluated, performance status, stage, histological grade and residual tumor size were significantly associated with disease-free and overall survival. The methylation status of Cyclin D2 was significantly associated with disease-free survival; the cases with methylation had significantly worse rates of disease-free survival than those without methylation (Fig. 6; $P = 0.021$). With

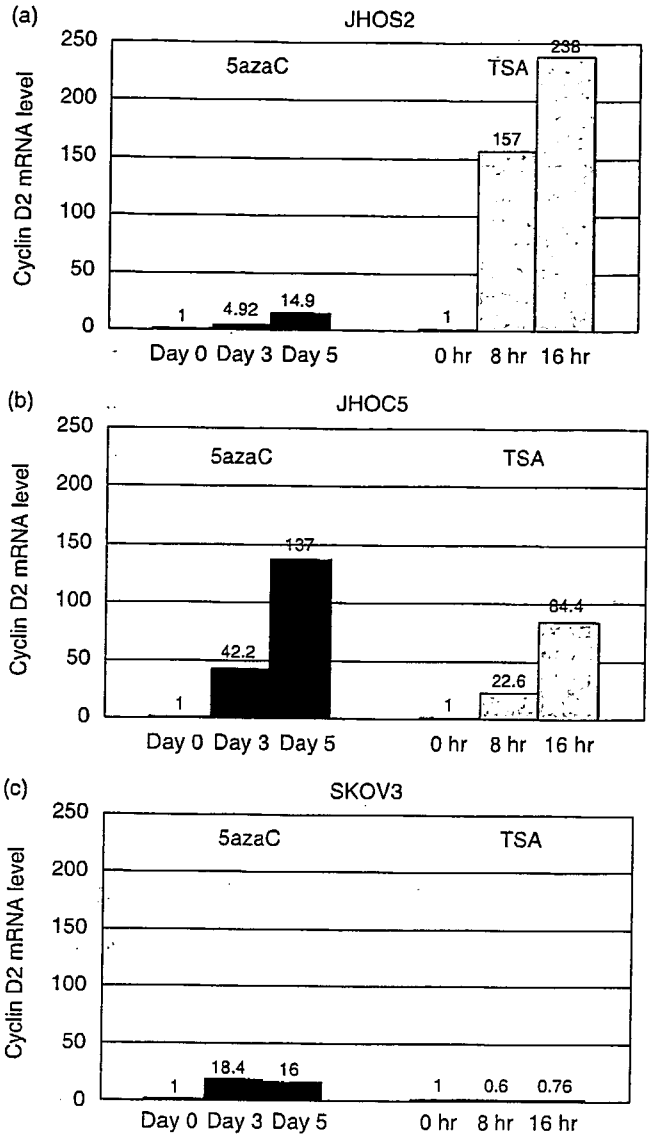


**Fig. 5.** Expression level of the Cyclin D2 gene as determined by quantitative reverse transcription–polymerase chain reaction in (a) JHOS2, (b) JHOC5 and (c) SKOV3 cells following treatment with 5-aza-2′-deoxycitidine (5azaC) or trichostatin A (TSA). The ratio of Cyclin D2 : β-actin was calculated and normalized with the level before treatment.

regard to overall survival, methylated cases had a worse prognosis than unmethylated cases, but the difference was not significant (Fig. 7; $P = 0.063$). In multivariate analysis, methylation status of cyclin D2 turned out not to be an independent prognostic factor (data not shown).

## Discussion

Aberrant promoter methylation is found in many types of human cancer and is a common mechanism for transcriptional inactivation of various genes, including tumor suppressor genes, DNA repair genes, cell cycle regulatory genes and apoptosis-related genes. In the present study, we determined the Cyclin D2 promoter methylation status of several ovarian cancer cell lines and ovarian cancer surgical specimens, measured the levels of Cyclin D2 gene expression in ovarian cancer cell lines and

**Table 2. Univariate analysis of disease-free survival**

| Variable | *P*-value |
|---|---|
| Cyclin D2 methylation status | 0.0212 |
| Age | 0.6657 |
| Performance status | <0.0001 |
| FigO stage | 0.0001 |
| Histological type | 0.4709 |
| Grade | 0.1332 |
| Residual tumor | 0.0008 |

**Table 3. Univariate analysis of overall survival**

| Variable | *P*-value |
|---|---|
| Cyclin D2 methylation status | 0.0625 |
| Age | 0.4195 |
| Performance status | 0.0003 |
| FigO stage | 0.0003 |
| Histological type | 0.0637 |
| Grade | 0.1983 |
| Residual tumor | 0.0016 |

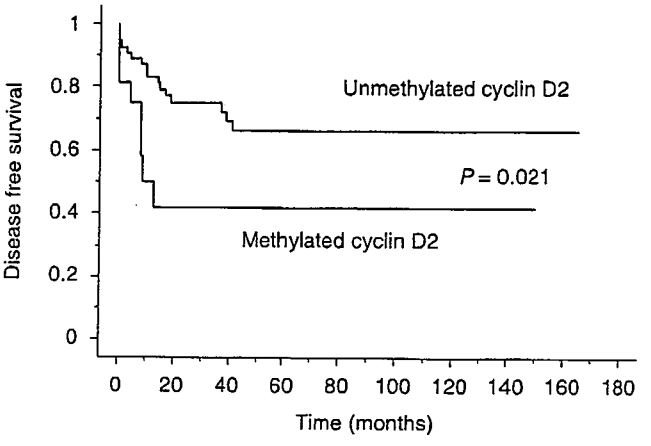


**Fig. 6.** Association between Cyclin D2 promoter methylation status and disease-free survival in patients with epithelial ovarian cancer.

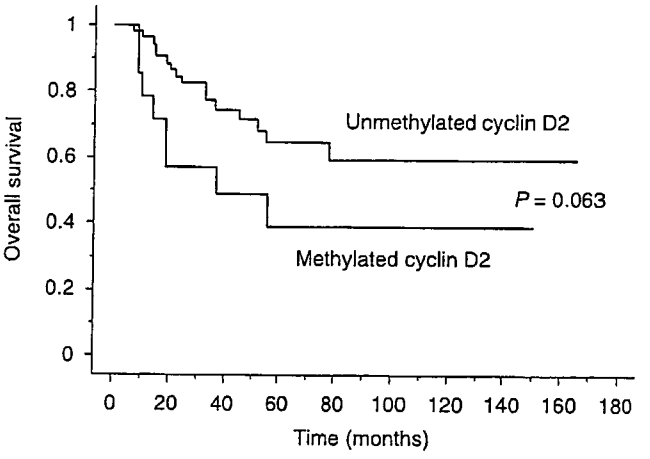


**Fig. 7.** Association between Cyclin D2 promoter methylation status and overall survival in patients with epithelial ovarian cancer.



doi: 10.1111/j.1349-7006.2007.00394.x

linked the methylation status of the Cyclin D2 promoter to various clinical and pathological variables in ovarian cancer patients.

From MSP and quantitative RT-PCR analysis, there was a trend towards a reduction in gene expression in the presence of hypermethylation; however, this association was not significant, and it was suggested that expression of the Cyclin D2 gene in ovarian cancer cell lines, as a whole, was considerably low in comparison with that in normal ovarian tissue. There was an increase in Cyclin D2 gene expression following the 5azaC treatment of cell lines with promoter methylation of the Cyclin D2 gene in MSP. However, TSA or 5azaC treatment of the cell lines without methylation in MSP resulted in re-expression of the Cyclin D2 gene. Together with these findings, it is suggested that some epigenetic changes, including promoter methylation or histone deacetylation, might contribute to silencing of the Cyclin D2 gene in epithelial ovarian cancer cell lines. The re-expression by treatment with 5azaC in the unmethylated cell lines JHOS2 and JHOC5 suggests that the Cyclin D2 gene may be secondary re-expressed owing to activating other suppressed gene by promoter methylation with treatment of 5azaC, or there is a possibility that aberrant methylation did exist but in a different region of the Cyclin D2 promoter to that which we analyzed. Further investigation and data regarding the acetylation status of histones, a different DNA methylation analysis to decipher the MSP results, and DNA methylation of the transcription factor of Cyclin D2 are needed to supplement our hypothesis.

Epithelial ovarian cancer cell growth following treatment with 5azaC or TSA was suppressed in OMC3 and OVCAR3 cell lines. Treatment with these chemical agents resulted in inhibition of cell growth as well as re-expression of the Cyclin D2 gene. However, another tumor suppressor gene was also re-expressed by these treatments, and these chemicals could have cell toxicity in itself[26–28]. The present data suggests that 5azaC and TSA could be therapeutic agents targeting epigenetic changes in epithelial ovarian cancer, and epigenetic gene silencing of the Cyclin D2 gene could used as a marker of tumor growth.

The D-type cyclins are early checkpoint regulators at the $G_1$ phase of the cell cycle. Although well known for their proliferation-promoting activity, the D-type cyclins also have growth-inhibitory effects.[14] Thus, decreased expression of Cyclin D2 could result in abnormal cell proliferation and contribute to malignant transformation. Indeed, Cyclin D2 gene silencing secondary to DNA promoter methylation has been demonstrated in several human cancers.[15–17,29] Cyclin D2 promoter hypermethylation has also been detected in nearly half of breast cancers and is associated with gene silencing. Cyclin D2 hypermethylation has also been demonstrated in small cell and non-small cell lung cancer tumor tissues and cell lines,[17] and in approximately half of gastric cancer specimens.[16] In the present study, 22.5% of the surgical specimens and 41.7% of the cell lines had aberrant Cyclin D2 promoter hypermethylation. Our results, though somewhat higher than what has been reported for ovarian granulosa cell tumors,[10] are similar to the percentages seen in several other cancers. Howver, some reports say that aberrant methylation of the Cyclin D2 promoter is an early event in tumorigenesis, as is suggested by its presence in ductal carcinoma *in situ* in breast cancer and its absence in normal ducts;[15,18,29] however, this epigenetic change was associated with advanced ovarian cancer in the present study. Our results suggest that aberrant methylation of this gene could be related to tumor progression rather than tumorigenesis of epithelial ovarian cancer.

A number of biological tumor variables, such as DNA ploidy, steroid hormone receptor status and the expression of certain oncogenes, are associated with prognosis in epithelial ovarian cancer.[30–32] The promoter methylation status of several genes, such as 14-3-3 sigma, BRCA1, hMLH1 and TMS1, has been used to predict poor survival in epithelial ovarian cancer patients.[9,24,33–35] In the present study, Cyclin D2 promoter methylation was significantly associated with advanced stage, a larger residual tumor size and poor prognosis. Because there was a trend toward the repression of gene expression in the presence of promoter hypermethylation in ovarian cancer cell lines, we presume that Cyclin D2 gene silencing might occur in primary tissues with methylation, though the levels of the Cyclin D2 gene have not been analyzed in this study. These results suggest that the aberrant promoter methylation of Cyclin D2, or decreased expression of this gene caused by methylation, may be associated with aggressive biological characteristics, and may play a significant role in disease progression in epithelial ovarian cancer.

The contribution of Cyclin D2 to the pathophysiology of epithelial ovarian cancer is not known at a rudimentary level. Though numerous studies have classified it as an oncogene, our data and that of others strongly supports the hypothesis that it functions as a tumor suppressor gene. Further studies are needed to better clarify the relationship between Cyclin D2 gene expression level and its function as either an oncogene or a tumor suppressor. A deeper understanding of the role of D-type cyclins in ovarian cancer tumor biology could provide a foundation on which to base new diagnostic tests or molecular therapies.

## Acknowledgment

We thank Setsuya Aiba (Department of Dermatology, Tohoku University Graduate School of Medicine) for technical assistance related to quantitative RT-PCR analysis.

## References

1 Akahira J, Yoshikawa H, Shimizu Y *et al.* Prognostic factors of stage IV epithelial ovarian cancer: a multicenter retrospective study. *Gynecol Oncol* 2001; **81**: 398–403.
2 Bonnefoi H, A'Hern RP, Fisher C *et al.* Natural history of stage IV epithelial ovarian cancer. *J Clin Oncol* 1999; **17**: 767–75.
3 Jones PA, Laird PW. Cancer epigenetics comes of age. *Nat Genet* 1999; **21**: 163–7.
4 Esteller M, Corn PG, Baylin SB, Herman JG. A gene hypermethylation profile of human cancer. *Cancer Res* 2001; **61**: 3225–9.
5 Kass SU, Pruss D, Wolffe AP. How does DNA methylation repress transcription? *Trends Genet* 1997; **13**: 444–9.
6 Razin A, Ceder H. DNA methylation and gene expression. *Microbiol Rev* 1991; **55**: 451–8.
7 O'Doherty AM, Church SW, Russell SHE *et al.* Methylation status of oestrogen receptor-α gene promoter sequences in human ovarian epithelial cell lines. *Br J Cancer* 2002; **86**: 282–4.
8 Rathi A, Virmani AK, Schorge JO *et al.* Methylation profiles of sporadic ovarian tumor and nonmalignant ovaries from high-risk women. *Clin Cancer Res* 2002; **8**: 3324–31.
9 Akahira J, Sugihashi Y, Suzuki T *et al.* Decreased expression of 14-3-3sigma is associated with advanced disease in human epithelial ovarian cancer: its correlation with aberrant DNA methylation. *Clin Cancer Res* 2004; **10**: 2687–93.
10 Dhillon VS, Shahid M, Husain SA. CpG methylation of the FHIT, FANCF, cyclin-D2, BRCA2 and RUNX3 genes in granulose cell tumors (GCTs) of ovarian origin. *Mol Cancer* 2004; **3**: 33.
11 Messague J. G1 cell-cycle control and cancer. *Nature* 2004; **432**: 298–306.
12 Zhang P. The cell cycle and development: redundant roles of cell cycle regulators. *Curr Opin Cell Biol* 1999; **11**: 655–62.
13 Sicinski P, Donaher JL, Geng Y *et al.* Cyclin D2 is an FSH-responsive gene involved in gonadal cell proliferation and oncogenesis. *Nature* 1996; **384**: 470–4.
14 Meyyappan M, Wong H, Hull C, Raibowol KT. Increased expression of cyclin D2 during multiple status of growth arrest in primary established cells. *Mol Cell Biol* 1998; **18**: 3163–72.

15 Evron E, Umbricht CB, Korz D *et al.* Loss of cyclin D2 expression in the majority of breast cancers is associated with promoter hypermethylation. *Cancer Res* 2001; **61**: 2782–7.
16 Yu J, Leung WK, Ebert MPA *et al.* Absence of cyclin D2 expression is associated with promoter hypermethylation in gastric cancer. *Br J Cancer* 2003; **88**: 1560–5.
17 Virmani A, Rathi A, Heda S *et al.* Aberrant methylation of the cyclin D2 promoter in primary small cell, nonsmall cell lung and breast cancers. *Int J Cancer* 2003; **107**: 341–5.
18 Fackler MJ, McVeigh M, Evron E *et al.* DNA methylation of RASSF1A, HIN-1, RAR-b, Cyclin D2 and Twist in *in situ* and invasive lobular breast carcinoma. *Int J Cancer* 2003; **107**: 970–5.
19 WHO. *Handbook for Reporting Results of Cancer Treatment*. WHO Publication No. 48. Geneva: WHO, 1979.
20 Shimizu Y, Kamoi H, Amada S *et al.* Toward the developing of a universal grading system for ovarian epithelial carcinoma. Prognostic significance of histopathologic features – problems involved in the architectural grading system. *Gynecol Oncol* 1998; **70**: 2–12.
21 Herman JG, Graff JR, Myohanen S *et al.* Methylation-specific PCR: a novel PCR assay for methylation status of CpG islands. *Proc Natl Acad Sci USA* 1996; **93**: 9821–6.
22 Choi DS, Yoon S, Lee EY *et al.* Characterization of cyclin D2 expression in human endometrium. *Gynecol Invest* 2002; **9**: 41–6.
23 Akahira J, Suzuki T, Ito K *et al.* Differential expression of progesterone receptor isoform A and B in the normal ovary, and in benign, borderline, and malignant ovarian tumors. *Jpn J Cancer Res* 2002; **93**: 807–15.
24 Akahira J, Sugihashi Y, Ito K *et al.* Promoter methylation status and expression of *TMS1* gene in human epithelial ovarian cancer. *Cancer Sci* 2004; **95**: 40–3.
25 Kamikihara T, Arima T, Kato K *et al.* Epigenetic silencing of the imprinted gene *ZAC* by DNA methylation is an early event in the progression of human ovarian cancer. *Int J Cancer* 2005; **115**: 690–700.
26 Schwartsmann G, Fernandes MS, Schaan MD *et al.* Decitabine (5-Aza-2′-deoxycytidine; DAC) plus daunorubicin as a first line treatment in patients with acute myeloid leukemia: preliminary observations. *Leukemia* 1997; **11**: S28–31.
27 Bender CM, Pao MM, Jones PA. Inhibition of DNA methylation by 5-aza-2′-deoxycytidine suppresses the growth of human tumor cell lines. *Cancer Res* 1998; **58**: 95–101.
28 Juttermann R, Li E, Jaenisch R. Toxicity of 5-aza-2′-deoxycytidine to mammalian cells is mediated primarily by covalent trapping of DNA methyltransferase rather than DNA demethylation. *Proc Natl Acad Sci USA* 1994; **91**: 11 797–801.
29 Evron E, Dooley WC, Umbricht CB *et al.* Detection of breast cancer cells in ductal lavage fluid by methylation-specific PCR. *Lancet* 2001; **357**: 1335–6.
30 Silvestrini R, Daidone MG, Veneroni S *et al.* The clinical predictivity of biomarkers of stage III–IV epithelial ovarian cancer in a prospective randomized treatment protocol. *Cancer* 1998; **82**: 159–67.
31 Akahira J, Inoue T, Suzuki T *et al.* Progesterone receptor isoforms A and B in human epithelial ovarian carcinoma: immunohistochemical and RT-PCR studies. *Br J Cancer* 2000; **83**: 1488–94.
32 Berchuck A, Kamel A, Whitaker R *et al.* Overexpression of HER-2/neu is associated with poor survival in advanced epithelial ovarian cancer. *Cancer Res* 1990; **50**: 4087–91.
33 Chiang JW, Karlan BY, Cass L, Baldwin RL. BRCA1 promoter methylation predicts adverse ovarian cancer prognosis. *Gynecol Oncol* 2006; **101**: 403–10.
34 Gifford G, Paul J, Vasey PA *et al.* The acquisition of hMLH1 methylation in plasma DNA after chemotherapy predicts poor survival for ovarian cancer patients. *Clin Cancer Res* 2004; **10**: 4420–6.
35 Terasawa K, SagaeS, Toyota M *et al.* Epigenetic inactivation of TMS1/ASC in ovarian cancer. *Clin Cancer Res* 2004; **10**: 2000–6.



doi: 10.1111/j.1349-7006.2007.00394.x

ELSEVIER

Bone 40 (2007) 876–887

BONE

www.elsevier.com/locate/bone

# Effects of aromatase inhibitors on human osteoblast and osteoblast-like cells: A possible androgenic bone protective effects induced by exemestane

Yasuhiro Miki [a], Takashi Suzuki [a], Masahito Hatori [b], Katsuhide Igarashi [c], Ken-ich Aisaki [c], Jun Kanno [c], Yasuhiro Nakamura [a], Miwa Uzuki [d], Takashi Sawai [c], Hironobu Sasano [a,*]

[a] *Department of Pathology, Tohoku University Graduate School of Medicine, 2-1 Seiryo-machi, Aoba-ku, Sendai, Miyagi, 980-8575, Japan*
[b] *Department of Orthopedic Surgery, Tohoku University Graduate School of Medicine, Sendai, Japan*
[c] *Division of Toxicology, National Institute of Health Sciences, Biological Safety Research Center, Setagaya, Tokyo, Japan*
[d] *Department of Pathology, Iwate Medical College, Morioka, Japan*

Received 21 April 2006; revised 6 November 2006; accepted 14 November 2006
Available online 28 December 2006

**Abstract**

Effects of aromatase inhibitors (AIs) on the human skeletal system due to systemic estrogen depletion are becoming clinically important due to their increasing use as an adjuvant therapy in postmenopausal women with breast cancer. However, possible effects of AIs on human bone cells have remained largely unknown. We therefore studied effects of AIs including the steroidal AI, exemestane (EXE), and non-steroidal AIs, Aromatase Inhibitor I (AI-I) and aminoglutethimide (AGM), on a human osteoblast. We employed a human osteoblast cell line, hFOB, which maintains relatively physiological status of estrogen and androgen pathways of human osteoblasts, i.e., expression of aromatase, androgen receptor (AR), and estrogen receptor (ER) β. We also employed osteoblast-like cell lines, Saos-2 and MG-63 which expressed aromatase, AR, and ERα/β in order to further evaluate the mechanisms of effects of AIs on osteoblasts. There was a significant increment in the number of the cells following 72 h treatment with EXE in hFOB and Saos-2 but not in MG-63, in which the level of AR mRNA was lower than that in hFOB and Saos-2. Alkaline phosphatase activity was also increased by EXE treatment in hFOB and Saos-2. Pretreatment with the AR blocker, flutamide, partially inhibited the effect of EXE. AI-I exerted no effects on osteoblast cell proliferation and AGM diminished the number of the cells. hFOB converted androstenedione into E2 and testosterone (TST). Both EXE and AI-I decreased E2 level and increased TST level. In a microarray analysis, gene profile patterns following treatment with EXE demonstrated similar patterns as with DHT but not with E2 treatment. The genes induced by EXE treatment were related to cell proliferation, differentiation which includes genes encoding cytoskeleton proteins. We also examined the expression levels of these genes using quantitative RT-PCR in hFOB and Saos-2 treated with EXE and DHT and with/without flutamide. HOXD11 gene known as bone morphogenesis factor and osteoblast growth-related genes were induced by EXE treatment as well as DHT treatment in both hFOB and Saos-2. These results indicated that the steroidal aromatase inhibitor, EXE, stimulated hFOB cell proliferation via both AR dependent and independent pathways.


*Keywords:* Osteoblast; Aromatase inhibitor; Androgen; Estrogen; Exemestane

## Introduction

Results in various epidemiological or clinical studies demonstrated that estrogens play important protective roles in human skeletal as well as cardiovascular systems, and estrogen deficiency resulted in accelerating the development of osteoporosis in postmenopausal women [1–3]. In breast cancer of postmenopausal women, hormone therapies without any clinically deleterious effects due to estrogen deficiency on bone metabolism as well as lipid metabolisms are preferable. Estrogen deficiency has been generally detected in the patients with breast cancer following chemotherapy induced ovarian failure, gonadotropin analogue, and aromatase inhibitors (AIs) therapy [4]. Aromatase is the pivotal enzyme of *in situ* or intratumoral estrogen biosynthesis in postmenopausal breast cancer patients, and catalyzes the conversion from androgens into estrogens (Fig. 1A). AIs therefore play an important role in

* Corresponding author. Fax: +81 22 273 5976.
*E-mail address:* hsasano@patholo2.med.tohoku.ac.jp (H. Sasano).

8756-3282/$ - see front matter © 2006 Elsevier Inc. All rights reserved.
doi:10.1016/j.bone.2006.11.029

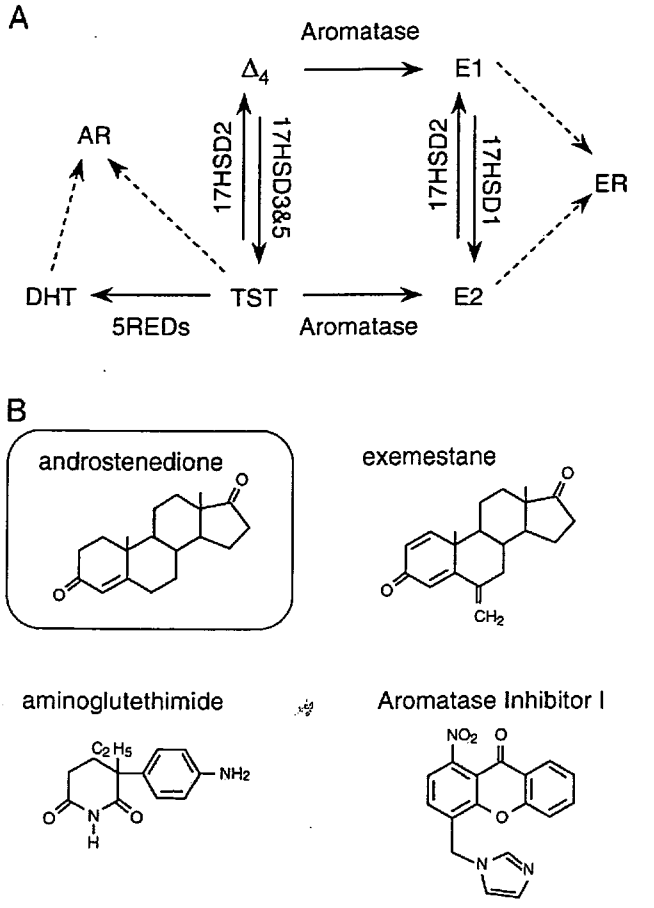


Fig. 1. (A) Summary of the pathway of estrogens and androgens production. Aromatase catalyzes the change from androstenedione (Δ4) and testosterone (TST) into estrone (E1) and estradiol (E2), respectively. 17HSD, 17β-hydroxysteroid dehydrogenase; 5REDs, 5α-reductase types 1 and 2; AR, androgen receptor; DHT, 5α-dihydrotestosterone; ER, estrogen receptor. (B) Structure of aromatase inhibitors used in this study. Androstenedione is a natural substrate of aromatase. Steroidal aromatase inhibitor, exemestane has an androstenedione-like structure.

clinical management of both primary and advanced breast cancer in postmenopausal women [5]. AIs are classified into two classes according to their modes of action. Type I AIs are steroidal inhibitions and one of them, exemestane (EXE) inhibits aromatase irreversibly and has an androstenedione ($\Delta_4$)-like structure (Fig. 1B) [5–7]. Type II AIs are non-steroidal inhibitions and include aminoglutethimide (AGM), anastrozole, and letrozole [5].

Results of *in vivo* study using ovariectomized (OVX) rats demonstrated that EXE and its principal metabolite form, 17-hydroexemestane (17H-EXE) but not letrozole significantly prevented bone loss in OVX rats [8,9]. EXE and its principal metabolite, 17H-EXE, are structurally related to $\Delta_4$ and bind to androgen receptor (AR) with relatively low affinity compared to 5α-dihydrotestosterone (DHT) [7]. These finding suggest that EXE may demonstrate protective effects toward bone tissues through its androgenic actions. However, detailed mechanisms of effects of EXE or androgen itself on human bone cells have remained largely unknown.

Various studies using human or animal bone tissues [10,11] and osteoblast cell culture using osteosarcoma cells [12,13] demonstrated that aromatase mRNA or protein was detected in osteoblast cells, which play an important role in bone remodeling. Therefore, in this study, we focused on effects of EXE in human osteoblast in an initial attempt to evaluate the effects of these AIs (summarized in Table 1 and Fig. 1B) [5–7,14], including AGM, EXE, and an experimental compound for inhibition of aromatase, Aromatase Inhibitor I (AI-I) [14] on human osteoblast and osteoblast-like cell lines. In our present study, we employed normal human cell line, hFOB, which maintains native characteristics of sex steroid hormone pathway of human osteoblasts, i.e., expression of AR, ERβ but not ERα, and aromatase. We also employed other osteoblast-like cell lines, Saos-2 and MG-63 which expressed ERα as well as ERβ in order to further study the mechanisms of effects of AI on human osteoblasts. We first examined the effects of estradiol (E2), DHT, progesterone (Prg), and AIs described above on cell proliferation of these cell lines, because the status of cell proliferation is important in the maintenance of homeostasis of bone tissue [15]. In addition, the effects of AIs on the conversion ratio of $\Delta_4$ into E2 or testosterone (TST) in hFOB cultured medium were examined. We then screened E2, DHT, and EXE responsive genes using a microarray analysis in these cells, in order to further characterize the possible genomic effects of EXE on cell proliferation of osteoblasts. In this microarray analysis, hFOB was employed in order to examine the effects of E2, DHT, and EXE on native status of human osteoblasts but not on pathological status of osteoblasts such as osteosarcomas.

## Materials and methods

### *Chemicals*

Exemestane (EXE; FCE24304; 6-methyleneandrosta-1,4-diene-3,17-dione) and 17-hydroexemestane (17H-EXE; FCE25071; 6-methyleneandrosta-1,4-diene-17β-ol-3-one) were obtained from Pfizer, Inc. (MI, USA). Aminoglutethimide (AGM) and Aromatase Inhibitor I [AI-I; 4-(Imidazolylmethyl)-1-nitro-9*H*-9-xanthenone] were obtained from Sigma-Aldrich Co. (MO, USA) and EMD Biosciences, Inc. (CA, USA), respectively. Estradiol (E2), progesterone (Prg), and RU38,486 (RU; mifepristone), spironolactone were obtained from Sigma-Aldrich. ICI 182,780 (ICI; fulvestrant) and hydroxyflutamide (OHF) were obtained from Tocris Cookson Inc. (MO, USA) and Toronto Research Chemicals, Inc. (Ontario, Canada), respectively. 5α-dihydrotestosterone (DHT) was obtained from Wako Pure Chemical industries, Ltd. (Osaka, Japan).

Table 1
Aromatase inhibitors used in this study

| | Aminoglutethimide | Exemestane | Aromatase inhibitor I |
|---|---|---|---|
| Trademark[a] | Cytadren® | Aromasin® | – |
| Type[b] | Type II | Type I | Type II |
| Generation | First | Third | – |
| IC50 (nM)[c] | 3000 | 50 | 40 |

[a] Cytadren® is trademark of Novartis Pharmaseutical Corporation. Aromasin® is trademark of Pfizer Inc. Aromatase Inhibitor I is non-clinical compound of Calbiochem®.

[b] Type I is steroidal compound. Type II is a non-steroidal compound.

[c] Refs, Aminoglutethimide and Exemestane are Miller et al. [5]; Aromatase Inhibitor I is Recanatini et al. [14].

These materials were dissolved in pure ethanol (Wako Pure Chemical industries) and serially diluted (final concentrations: $10^{-12}$ M to $10^{-5}$ M), respectively. AGM was dissolved in DMSO (Wako Pure Chemical industries). The final concentration of ethanol and DMSO used in this study did not exceed 0.05%.

### *Osteoblast cell and osteoblast-like cell lines and culture conditions*

Human normal osteoblast cell, hFOB 1.19 cell line (CRL-11372) was obtained from American Type Culture Collection (VA, USA). hFOB 1.19 cell was cultured according to the protocol previously described [16]. The cell line was maintained in a mixture of Dulbecco's Modified Eagle Medium and Ham's F12 medium (1:1) without phenol red (Invitrogen Corporation, CA, USA) supplemented with 10% fetal bovine serum (FBS; JRH Biosciences, KS, USA) and 50 mg/mL G 418 sulfate (EMD Biosciences). Human osteosarcoma cell lines Saos-2 and MG-63 were provided from the Cell Resource Center for Biomedical Research, Tohoku University (Sendai, Japan) and were maintained in a RPMI-1640 (Sigma-Aldrich) with 10% FBS. These cells were pre-incubated for 24 h with FBS-free medium prior to examination in order to remove exo-/endogenous steroid hormones from the culture medium and study the effects of various compounds in the absence of steroids and also to synchronize the cell cycle. Different concentrations of test compounds were added, and the assay was terminated after 3 or 5 days by removing the medium from wells. Steroid blockers were added simultaneously.

### *Characteristics of hFOB, Saos-2, and MG-63*

Expressions of relevant steroid receptors, i.e., ERα, ERβ, and AR were determined using quantitative RT-PCR methods in hFOB, Saos-2, and MG-63 cell lines. mRNA transcripts of steroid synthesis/metabolite enzymes, aromatase, 17β-hydroxysteroid dehydrogenase (17β-HSD) types 1, 2, 3, 4, and 5, and 5α-reductase (5α-Red) types 1 and 2 were all evaluated using RT-PCR methods. The details of quantitative RT-PCR including primer sets employed were previously described in detail [17,18]. Positive controls for these receptors and enzymes were cell lines of human breast cancer, T-47D, and human prostate cancer, LNCaP obtained from Cell Resource Center for Biomedical Research, Tohoku University (Sendai, Japan). Alkaline phosphatase (ALP), an osteoblast-specific marker, was also studied using RT-PCR for characterization of these cell lines.

### *Estradiol and testosterone production assay*

hFOB cells were plated in 10 mm dishes at a density of $10^6$ viable cells and cultured for 48 h. Then media were changed to FBS-free medium, and hFOB cells were incubated with $10^{-7}$ M androstenedione ($\Delta_4$; Sigma-Aldrich) in the presence or absence of EXE or AI-I ($10^{-7}$ M). The media were then collected after 24 h, and E2 and TST were measured by solid-phase radioimmunoassay. Radioimmunoassay was performed in SRL Inc. (Tokyo, Japan) using DPC estradiol kit and DPC total testosterone kit (Diagnostic Products Corporation, LA, USA). In addition, we confirmed that the concentrations of E2 and TST were under the detection limits (E2, 5 pg/mL; TST, 30 pg/mL) in the serum- and phenol red-free medium.

### *Cell proliferation assay*

hFOB, Saos-2, and MG-63 cells were treated with steroids and test compounds for 24, 48, and 72 h, when specimens were harvested and evaluated for cell proliferation using the WST-8 method (Cell Counting Kit-8; Dojindo Inc., Kumamoto, Japan) [18]. Optical densities (OD, 450 nm) were evaluated using a SpectraMax 190 microplate reader (Molecular Devices, Corp., CA, USA) and Softmax Pro 4.3 microplate analysis software (Molecular Devices). The status of proliferation (%) was calculated according to the following equation: (cell OD value after test materials treated/vehicle control cell OD value) × 100.

### *Alkaline phosphatase activity assay*

hFOB, Saos-2, and MG-63 cells were plated in 48 well plate at a density of $10^6$ viable cells and cultured for 48 h. All cell lines were treated with $10^{-9}$ to $10^{-7}$ M exemestane for 72 h, when cells were lysed with 0.05% Triton X-100 (Wako Pure Chemical industries) and evaluated for alkaline phosphatase activity

Table 2
Primer sequences used in quantitative RT-PCR analysis

| cDNA | GB# | Sequence | cDNA position | Size (bp) |
|---|---|---|---|---|
| MYBL2 | NM_002466 | Forward 5′-GTAACAGCCTCACGCCCAAGA-3′<br>Reverse 5′-TCCAATGTGTCCTGTTTGTTCCA-3′ | 1522–1615 | 94 |
| OSTM1 | NM_014028 | Forward 5′-TTGAGAATAAGGCTGAACCTGGAAC-3′<br>Reverse 5′-TTACAGGCACTGTGTCACTGCAAG-3′ | 801–926 | 126 |
| HOXD11[a] | NM_021192 | Forward 5′-CAC TGT CCT TGG GTT TAA TG-3′<br>Reverse 5′-GGT AAA ATT GTA ACG GGA CG-3′ | 1091–1245 | 174 |
| GPC2 | NM_152742 | Forward 5′-AGA AAT GTG GTC AGC GAA GC-3′<br>Reverse 5′-ACA CCT TCG CAC TGT TTT CC-3′ | 871-1183 | 313 |
| ADCYAP1R1 | NM_001118 | Forward 5′-CAG CAA AAG GGA AAG ACT CG-3′<br>Reverse 5′-GAG CTG CTC TTG CTC AGG AT-3′ | 1351–1584 | 234 |
| COL1A1 | NM_000088 | Forward 5′-GGT GGT GGT TAT GAC TTT GGT T-3′<br>Reverse 5′-CTT GGC TGG GAT GTT TTC AGG T-3′ | 3784–4092 | 309 |
| SMAD1[a] | NM_005900 | Forward 5′-GGT TCA CCT CAT AAT CCT-3′<br>Reverse 5′-CCT TTG TCA GTT CTC AAT C-3′ | 1779–1887 | 127 |
| SMAD5[a] | NM_005903 | Forward 5′-AGC TAA AGC CGT TGG ATA-3′<br>Reverse 5′-AGG CAC TAA TAC TGG AGG T-3′ | 668–768 | 119 |
| RUNX2 | NM_004348 | Forward 5′-GTG GAC GAG GCA AGA GTT T-3′<br>Reverse 5′-TAC TGG GAT GAG GAA TGC G-3′ | 782–961 | 198 |
| SPARC | NM_003118 | Forward 5′-CCT GTA CAC TGG CAG TTC-3′<br>Reverse 5′-CCA GGG CGA TGT ACT TGT C-3′ | 793–937 | 163 |
| ALP | NM_000478 | Forward 5′-ACC ATT CCC ACG TCT TCA CA-3′<br>Reverse 5′-AGA CAT TCT CTC GTT CAC CGC C-3′ | 1379–1540 | 162 |
| RPL13A | NM_012423 | Forward 5′-CCT GGA GGA GAA GAG GAA AGA GA-3′<br>Reverse 5′-TTG AGG ACC TCT GTG TAT TTG TCA A-3′ | 487–612 | 126 |

GB#, GeneBank accession number.
All primer sets were designed using OLIGO Primer Analysis Software (TAKARA Bio Inc., Shiga, Japan).
[a] Forward and reverse primers were located in sama exon.

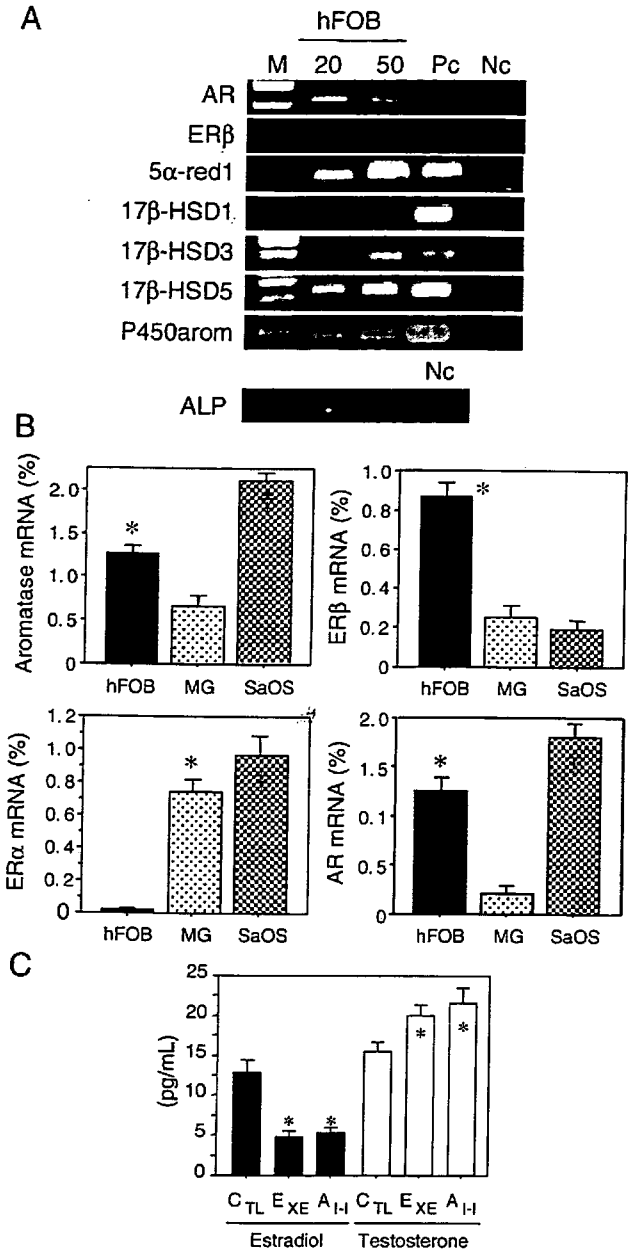


Fig. 2. (A) Results of RT-PCR analysis of steroid hormone receptors and steroid-related enzymes. Both 20 and 50 ng/μL cDNA of hFOB were used for PCR (ALP was 20 ng/μL alone). AR, androgen receptor; ER, estrogen receptor; 5α-red1, 5α-reductase type 1; 17β-HSD, 17β-hydroxysteroid dehydrogenase; P450 arom, aromatase; M, molecular marker; Pc, positive control; Nc, negative control. (B) Expression levels of aromatase, AR, ERα, and ERβ in hFOB, Saos-2, and MG-63. *$p<0.05$ vs. MG-63 (aromatase and AR), vs. MG-63 and vs. Saos-2 (ERβ), vs. hFOB (ERα); †$p<0.05$ vs. hFOB and MG-63 (aromatase and AR), vs. MG-63 and hFOB (ERα). (C) Estradiol and testosterone productions in hFOB cells. The data are expressed as the mean SD ($n=3$). *$p<0.05$ vs. control cells (CTL). EXE, $10^{-7}$ M exemestane; AI-I, $10^{-7}$ M aromatase inhibitor I.

using the *p*-nitrophenylphosphate method (LabAssay ALP; Wako Pure Chemical industries) [19]. Optical densities (OD, 405 nm) were evaluated using a SpectraMax 190 microplate reader (Molecular Devices) and Softmax Pro 4.3 microplate analysis software (Molecular Devices). ALP activity (units/μL)=(concentration of *p*-nitrophenol/15 min)×1 (dilution factor of sample). The ALP activities were presented as units/μL/$10^6$ cells. The ALP activity levels in each case were represented as a ratio of vehicle control (%).

### *Microarray analysis*

The procedure was based on a previously reported study [20]. Cell lysates were prepared using RLT buffer (QIAGEN GmbH, Hilden, Germany). Total RNA was extracted using RNeasy Mini Kit (QIAGEN). First-strand cDNA was synthesized by incubating 5 μg of total RNA with 200 U SuperScript II reverse transcriptase (Invitrogen), 100 pmol T7-(dT)24 primer (Invitrogen). Ten units of T4 DNA polymerase (Invitrogen) were then added, and the dsDNA was mixed with T7 RNA polymerase (Invitrogen). The purified cRNA was fragmented at 300–500 bp as target solution. Hybridization was performed with the GeneChip Human Genome 133 ver. 2.0 (Affymetrix, Inc., CA, USA). The reacted arrays were then scanned as digital image files and scanned data were analyzed with GeneChip software (Affymetrix). Relative levels of gene expression were calculated by global normalization.

Data were subjected to hierarchical clustering analysis and visualization using the Cluster and TreeView programs (Stanford University) in order to generate tree structures based on the degree of similarity, as well as matrices comparing the levels of expression of individual genes in each sample [21].

### *Real-time PCR*

Real-time PCR was carried out using the LightCycler System and the FastStart DNA Master SYBR Green I (Roche Diagnostics GmbH, Mannheim, Germany). The primer sequences used in this study are summarized in Table 2. An initial denaturing step of 95 °C for 10 min was followed by 35 cycles, respectively, at 95 °C for 10 min; 15 s annealing at 65 °C (ALP, COL1A1), 64 °C (MYBL2, OSTM1, RPL13A), 62 °C (SMAD1, SMAD5, SPARC, RUNX2), or 60 °C (HOXD11); and extension for 15 s at 72 °C. Negative control experiments included those lacking cDNA substrates to confirm the presence of exogenous contaminant DNA. No amplified products were detected under these conditions. The mRNA levels in each case were represented as a ratio of RPL13A (%) [22].

### *Immunohistochemistry of AR*

Five non-pathological bone tissues were retrieved from surgical pathology files (two females and three males, 17 to 55 years old) of Department of Pathology, Tohoku University Hospital (Sendai, Japan).

Tissue sections were immunostained using a biotin-streptavidin method with Histofine kit (Nichirei Co. Ltd., Tokyo, Japan). The monoclonal antibody for AR (AR411) [23] was obtained from DakoCytomation (Kyoto, Japan). Experimental procedures employed in our present study have been previously described in detail [22,23]. The dilutions of primary AR antibody were 1:100. The antigen-antibody complex was then visualized with 3,3′-diaminobenzidine solution, and counterstained with hematoxylin. Prostate cancer was used as a positive control for AR. Normal mouse IgG was used as a negative control for immunostaining and no specific immunoreactivity was detected.

### *Statistical analysis*

Results were expressed as mean±SD. Statistical analysis was performed with the StatView 5.0 J software (SAS Institute Inc., NC, USA). All data were analyzed by analysis of variance (ANOVA) followed by post hoc Bonferroni/Dunnett multiple comparison test. A $p$-value$<0.05$ was considered to indicate statistical significance.

## Results

### *Characteristics of hFOB, MG-63, and Saos-2 cell line*

Characteristics of osteoblast and osteoblast-like cell lines are summarized in Figs. 2A and B. hFOB cells expressed mRNA transcripts of AR and ERβ. Relatively low level of ERα mRNA transcript was detected in hFOB cells. Aromatase, 17β-HSD type 1, 3, and 5, and 5α-Red types 1 and 2 mRNA transcripts were all detected in hFOB cells by

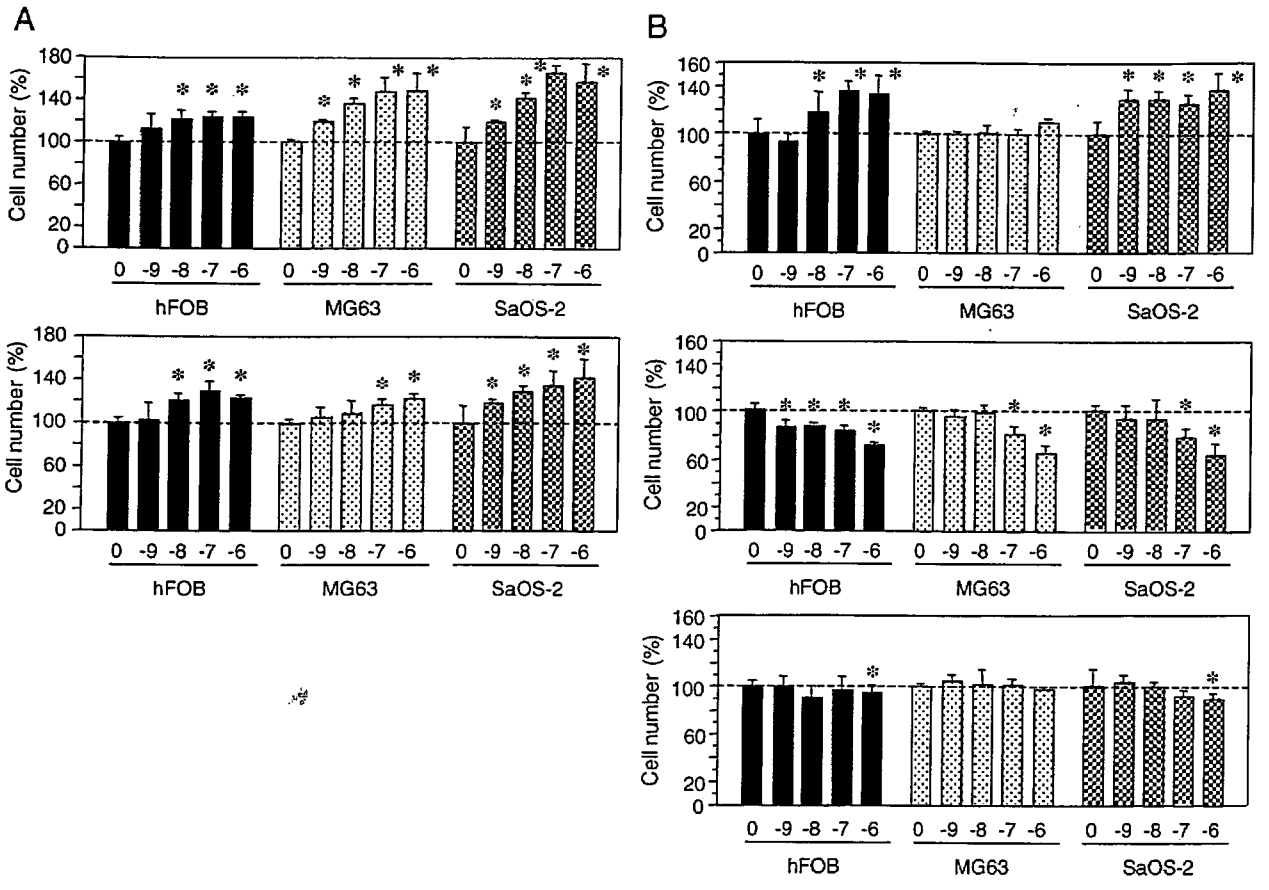


Fig. 3. (A) Proliferation of hFOB cells treated by estradiol (top) and 5α-DHT (bottom). *$p<0.05$ vs. vehicle control (0). (B) Proliferation of hFOB cells treated by exemestane (top), aminogluthetimide (middle), and Aromatase Inhibitor-I (bottom). *$p<0.05$ vs. vehicle control (0). $n=5$.

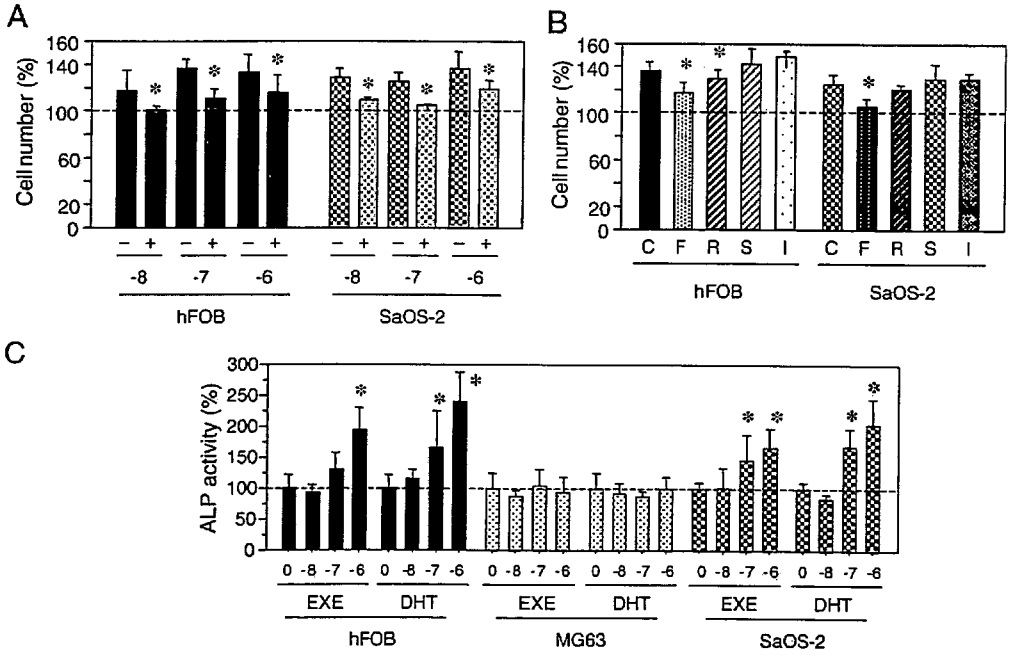


Fig. 4. (A) Effects of hydroxyflutamide on exemestane ($10^{-8}$ to $10^{-6}$ M) stimulated the cell proliferation of both hFOB and Saos-2. With (+) or without (−) hydroxyflutamide, $p<0.05$ vs. without hydroxyflutamide (*). (B) Effects of steroid receptor blockers on exemestane ($10^{-7}$ M) stimulated cell proliferation of hFOB and Saos-2. C, $10^{-7}$ M exemestane; F, hydroxyflutamide ($5\times10^{-6}$ M); R, RU38,486 ($5\times10^{-6}$ M); S, spironolactone ($5\times10^{-6}$ M); I, ICI182,720 ($5\times10^{-6}$ M). *$p<0.05$ vs. C (C) ALP activity in hFOB, Saos-2, MG-63 treated with exemestane (EXE, $10^{-8}$ to $10^{-6}$ M), or 5α-DHT (DHT, $10^{-8}$ to $10^{-6}$ M). *$p<0.05$ vs. vehicle control (0).